

GEOLOGY STUDIES

Volume 19: Part 2 — December 1972

CONTENTS

Lateral Facies and Paleocology of Permian Elephant Canyon Formation, Grand County, Utah	Forrest M. Terrell	3
Paleocology and Paleoenvironments of the Upper Honaker Trail Formation near Moab, Utah	Robert A. Melton	45
Sedimentary Features and Paleoenvironment of the Dakota Sandstone (Early Upper Cretaceous) near Hanksville, Utah	Gary Frank Lawyer	89
Recent History of Utah Lake as Reflected in Its Sediments: A First Report	Willis H. Brimhall	121
Pennsylvanian Sponges from the Oquirrh Group of Central Utah	J. Keith Rigby and A. Jaren Swensen	127
Shoshonitic Lavas in West-Central Utah	Norman C. Hogg	133
Publications and maps of the Geology Department		185

Brigham Young University Geology Studies

Volume 19, Part 2 — December 1972

Contents

Lateral Facies and Paleocology of Permian Elephant Canyon Formation, Grand County, Utah	Forrest M. Terrell	3
Paleocology and Paleoenvironments of the Upper Honaker Trail Formation near Moab, Utah	Robert A. Melton	45
Sedimentary Features and Paleoenvironment of the Dakota Sandstone (Early Upper Cretaceous) near Hanksville, Utah	Gary Frank Lawyer	89
Recent History of Utah Lake as Reflected in Its Sediments: A First Report	Willis H. Brimhall	121
Pennsylvanian Sponges from the Oquirrh Group of Central Utah	J. Keith Rigby and A. Jaren Swensen	127
Shoshonitic Lavas in West-Central Utah	Norman C. Hogg	133
Publications and maps of the Geology Department		185

A publication of the
Department of Geology
Brigham Young University
Provo, Utah 84601

Editor

J. Keith Rigby

Brigham Young University Geology Studies is published semiannually by the department. *Geology Studies* consists of graduate student and staff research in the department and occasional papers from other contributors.

Distributed December 22, 1972

Price \$4.00

Paleoecology and Paleoenvironment of the Upper Honaker Trail Formation Near Moab, Utah

ROBERT A. MELTON

Department of Geology, University of South Carolina, Columbia, S. C. 29208

ABSTRACT.—A single section of rocks, 600 feet thick, in the upper Honaker Trail Formation south of U.S. Highway 160 across from Arches National Park Headquarters near Moab, Utah, was studied for sedimentary structures, lithology, fauna, geochemistry, and sequences of beds.

Clastic rocks present in the principal and auxiliary sections are (1) coarse- and fine-grained purple and white arkoses containing tabular and trough cross-bedding, megaripples, and trace fossils; (2) fine-grained and very fine-grained orange and white sandstones containing tabular cross-bedding, flat-bedding, mudcracks, ripple marks and trace fossils; and (3) silty, maroon and gray shale with a gastropod-dominated fossil assemblage. Clastic sediments were derived from the Uncompahgre Uplift to the east and northeast.

Carbonate rocks present include (1) sparry dolomite, usually highly bioturbated; (2) micritic limestone containing fossil assemblages dominated by corals, brachiopods, mollusks, algae, and trace fossils; and (3) sandy limestone containing repichnid trace fossils.

Deposits represent various sedimentary environments, including delta lobes, longshore bars, tidal flats, lagoons, and open-marine environments.

Rocks of the sequence show evidence of arid climate with minor pulses that quickly deposited arkosic deltas. Longshore currents reworked arkoses of delta lobes to produce longshore bars. Tidal flats and carbonate mud lagoons developed adjacent to and behind delta and bar deposits. Open-marine carbonate deposits existed offshore with diverse and dense stable fossil communities.

A hypothetical sedimentary model infers that numerous migrating delta complexes prograded out from the Uncompahgre Uplift flanks into the Paradox Basin. Individual deltas were abandoned and buried by open marine-carbonate deposits in transgressive stages; however, delta complexes eventually migrated back again and produced repetitive sedimentation.

CONTENTS

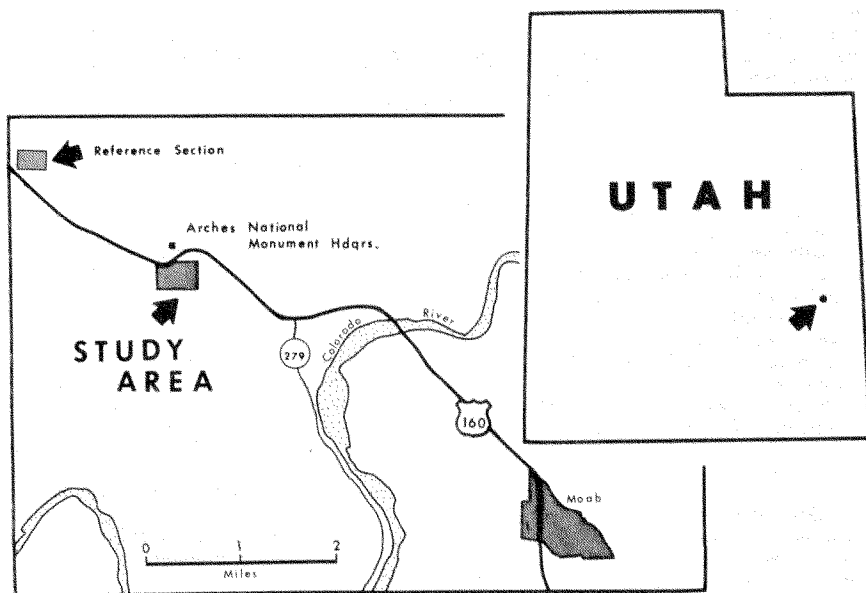
TEXT	page		
Introduction	46	Climate and general conditions	76
Purpose	47	Fossil habitats and relationships	79
Geologic setting	48	Sedimentary environments	80
Location and physical		Sedimentary model	83
characteristics	48	Summary	85
Field methods and laboratory		Appendix (measured section)	85
techniques	48	References cited	88
Previous work	49		
Acknowledgments	50	ILLUSTRATIONS	
Stratigraphic subdivisions	50	Text-figures	
Clastic rocks	50	1. Index map showing location of	
Carbonate rocks	54	studied area and auxiliary refer-	
Invertebrate fossils	58	ence section north of Moab,	
Corals	65	Grand County, Utah	46
Brachiopods	67	2. Isopach map of Honaker Trail	
Mollusks	68	Formation and location of stud-	
Miscellaneous fossils	71	ied area	47
Sequence of fossils	72	3. Total studied stratigraphic sec-	
Trace fossils	72	tion showing lithology and sedi-	
Geochemistry	75	mentary structures	51

*A thesis presented to the Department of Geology, Brigham Young University, in partial fulfillment of the requirements for the degree Master of Sciences, August 1972.

4. Stratigraphic column of selected clastic units, showing variations in lithology, sedimentary structures, grain size and paleocurrent direction	52	10. Sedimentary model of delta complex and carbonate environments with superimposed distribution of sedimentary structures	84
5. Selected carbonate units, showing percentage of total fauna compared to matrix and percentage of selected fauna compared to total fauna	59	Plates	
6. Selected carbonate units showing percentage of selected genera compared to total fauna	66	1. Fields views	55
7. Distribution and ratios of trace elements in selected carbonate units	77	2. Field views of rock units	57
8. Diagram of rock units in studied section with superimposed sedimentary environments	81	3. Photomicrographs of clastic rocks	61
9. Sedimentary model showing hypothetical delta complex and laterally equivalent marine carbonates with fossil distribution superimposed	82	4. Photomicrographs of limestones	62
		5. Corals, gastropods, and other fossils	63
		6. Brachiopods, bivalves, and bryozoans	69
		7. Brachiopods	70
		8. Trace fossils	73
		Tables	
		1. Distribution of fossil species in studied section	64
		2. Geochemical results of selected units in studied section	75

INTRODUCTION

The upper Honaker Trail Formation of the Paradox Basin is a cyclically deposited sequence of carbonate rocks and redbeds. It is well exposed at the study locale near Moab, in eastern Utah (Text-fig. 1), and is paleogeographical-



TEXT-FIGURE 1.—Index map, showing location of studied area and auxiliary reference section north of Moab, Grand County, Utah.

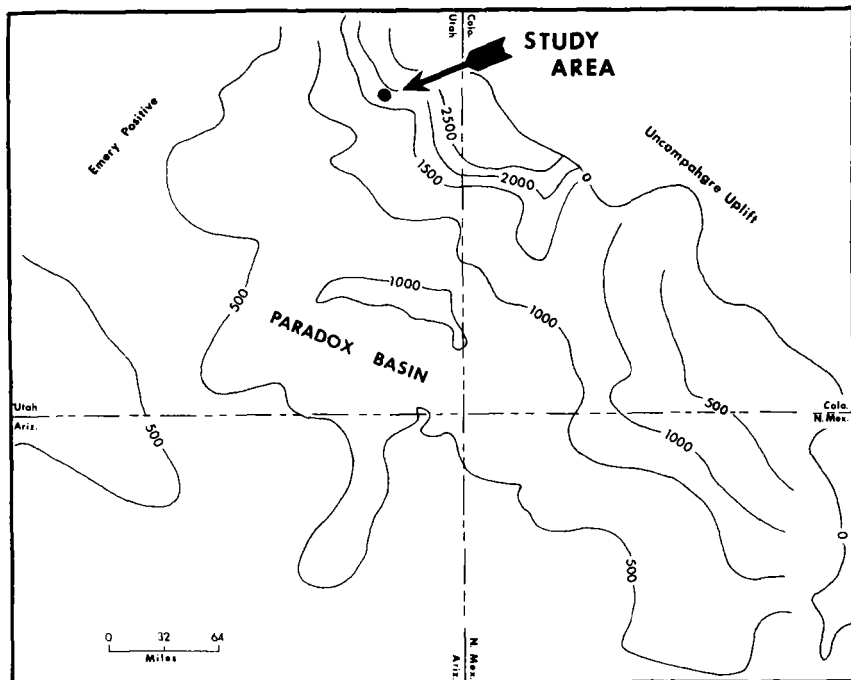
ly situated in the northern middle of the Paradox Basin. The area studied is 40 to 60 miles west of the Uncompahge Uplift (Text-fig. 2) and approximately 100 miles east of the Emery Uplift. The Honaker Trail Formation in this region is between 1,500 and 2,000 feet thick (Wengerd, 1962, p. 316). The sequence is excellent for paleoecological study because it shows numerous environments of deposition in one locale. Careful analysis of these strata has provided data to formulate a model interpreting the paleoecology and sedimentary environment.

Specifically, this investigation describes and documents the geochemistry (carbonates only), lithologies, sedimentary structures, paleocurrents, faunal assemblages, faunal density and diversity, faunal-sediment associations, and repetitive nature of a single section of the upper Honaker Trail Formation.

From these data, interrelationships concerning the paleoecology and sedimentary environment are interpreted. Environmental parameters considered include climate; water temperature, depth, salinity, and turbidity; current direction and velocity; and fossil communities.

PURPOSE

As structural traps containing profitable amounts of oil are becoming more difficult to find, the importance of finding stratigraphically trapped oil is increasing. The above-mentioned parameters were documented in order to construct



TEXT-FIGURE 2.—Isopach map of Honaker Trail Formation (Wengerd, 1962, p. 316) and location of studied area.

a sedimentary model which may be useful in the search for stratigraphically trapped petroleum.

GEOLOGIC SETTING

During the Middle Pennsylvanian, the Paradox Basin began to subside. Prior to this the area was part of the stable shelf east of the Cordilleran miogeosyncline. With the rise of the bordering Zuni, Emery, and Uncompahgre-San Luis uplifts, it was isolated from the main shelf. Circulation into the basin was restricted at times, resulting in the deposition of dark shale, gypsum, and salt, such as is found in the Paradox Formation (Wengerd, 1962, p. 264). During the Late Pennsylvanian, cyclic sediments of the Honaker Trail Formation were deposited in the basin as the Uncompahgre Uplift rose and shed large quantities of arkosic sediment along the basin margin. Concurrently, intrabasin tectonic activity and evaporites from the underlying Paradox Formation disrupted basin geometry (Wengerd, 1962, p. 301). As a result of the rapid influx of arkosic sediment, the Honaker Trail Sea began to retreat. By the Middle Permian, predominantly clastic sediment from the Cutler Formation covered the basin.

The change from marine to nonmarine deposition, the environmental processes, and the conditions under which the regression took place will be dealt with in this paper.

LOCATION AND PHYSICAL CHARACTERISTICS

The study locale is southwest, across U.S. Highway 160 from Arches National Park Headquarters, $5\frac{1}{2}$ miles northwest of Moab, Grand County, Utah (Text-fig. 1). It is in Sections 20 and 21, T. 25 S., R. 21 E. The principal section is traversed by the Denver and Rio Grande Western Railroad. Northwest- and southwest-trending gullies give best rock exposures. An auxiliary reference section was studied in a gully parallel to the old highway, 2 miles northwest of the principal section, in Section 18, T. 25 S., 21 E.

Both the principal and auxiliary sections are on the southwestern limb of the Moab Anticline in Moab Canyon. Both include rocks of Pennsylvanian to probable Permian age. The principal section is approximately 600 feet thick and is unconformably capped by the Moenkopi Formation but is cut at its base by the Moab Fault.

Rock types include limestone, dolomite, silty shale, quartzitic sandstone, and arkosic, conglomeratic sandstone. Long dip slopes provide excellent surfaces for fossil collecting and counting. Excellent exposures of every unit are available within the principal and auxiliary sections. Most of the field work was done on the south side of the large railway fill because of better exposures and because fewer "rock hounds" have collected in the area.

FIELD METHODS AND LABORATORY TECHNIQUES

The section was measured with a Brunton Compass and a steel tape or six-foot ruler. Units 1 through 10 were measured and sampled on the north side of the large railway fill; units 11 through 26, on the south side. Over 150 thin sections were made. Unconsolidated samples were impregnated with epoxy resin before sectioning. Twenty samples, whose lo-

cations are shown in Table 2, were collected from carbonate units for geochemical analysis.

Twenty-two samples of approximately 1,000 grams each were collected for conodonts from carbonate units. They were crushed and etched in a ten-percent solution of acetic acid. Undissolved material was washed on a one-hundred mesh screen, dried, and examined under a binocular microscope. No microfossils were recovered.

Fossils were collected from talus and bedrock. Those found in talus were correlated with the measured section according to lithology, location, and faunal associations. Fossil density and diversity were measured on numerous bedding-plane surfaces using a grid 1 foot wide, 2 feet long, and divided into one-inch squares. Fossil fragments were included but were not distinguished from whole fossils. Each grid intersection was counted as either fossil or matrix. Each fossil was then identified, where possible, on the species level. Approximately 200 square feet of bedding-plane surface were covered in units 7, 11, 13, 14, and 15, representing most available fossiliferous outcrops. Data reveal the amount of space occupied by the fossil populations compared to that occupied by the matrix, and the amount of space occupied by each phylum and genus compared to that occupied by the total faunal population of each bedding-plane surface. Relationships were calculated in percentages for total faunal/matrix, selected phylum/total fauna, and selected genera/total fauna.

Over 200 paleocurrent directions were measured with a Brunton Compass on a unit-by-unit basis. Rose diagrams and sketch maps were constructed from these measurements. Arrow vectors for sketch maps were constructed graphically from clusters of readings.

Carbonates were boiled in a solution of NaOH and Alizarin Red S to test for dolomite (Friedman, 1959). Clastics were soaked in HF acid and stained with a Potassium cobaltinitrate solution to test for feldspars. To aid in identification, acetate peels were made from most of the corals collected.

PREVIOUS WORK

Formation names which have been applied to the studied area include "Cutler," "Rico," and "Hermosa." Baars (1962) believes the Rico Formation of the studied area should be included in the Honaker Trail Formation because the Rico facies is a localized phenomenon.

The Cutler Formation was named by Cross and Howe (1905, p. 461). Spencer defined the Rico Formation which was later described by Cross (1899, p. 3). In 1899, Spencer also named the Hermosa Formation. The "Honaker Trail Formation," named by Wengerd and Matheny (1958, p. 2075-80), replaces the former "upper Hermosa Formation."

Numerous fossil collections have been gathered from the studied area in the past. The first was by Newberry (1876, p. 98), who was followed by Prindle in 1901 and Cross in 1905. These collections and many from other sites were assembled by Cross in 1907 (p. 672) for correlation purposes. Baker (1927, p. 792-793) assembled fossil lists which differentiate Pennsylvanian and Permian faunas in the studied area and in the Moab region generally. Baker and Girty collected fossils on a layer-by-layer basis, noting approximately where fossil groups were located in the studied locale. Baker

(1933) tabulated fossil locations for the Moab region, including the studied locale. Chronic (1960, p. 80) published fossil lists from the literature which included the studied locale.

Baars (1962, p. 159) reported that "along the fault zone north of Moab, Cutler red beds equivalent to Wolfcamp carbonates on the west overlie the limestones containing Virgil fusulinids."

Parr (1955) did a general study of paleocurrent direction in Moab Canyon north of Arches National Park Headquarters.

ACKNOWLEDGMENTS

Sincere thanks is given to Dr. J. K. Rigby for serving as committee chairman and Drs. W. K. Hamblin and H. J. Bissell for serving as committee members. Union Oil Company of California provided financial support for the study. Special gratitude is given to Sharon, my wife, who helped with the drafting, editing, typing, thin-section preparation, and field work. Thanks are given to Gary Lawyer for doing the geochemical laboratory work and to other graduate students at Brigham Young University whose opinions and equipment they often shared with the writer.

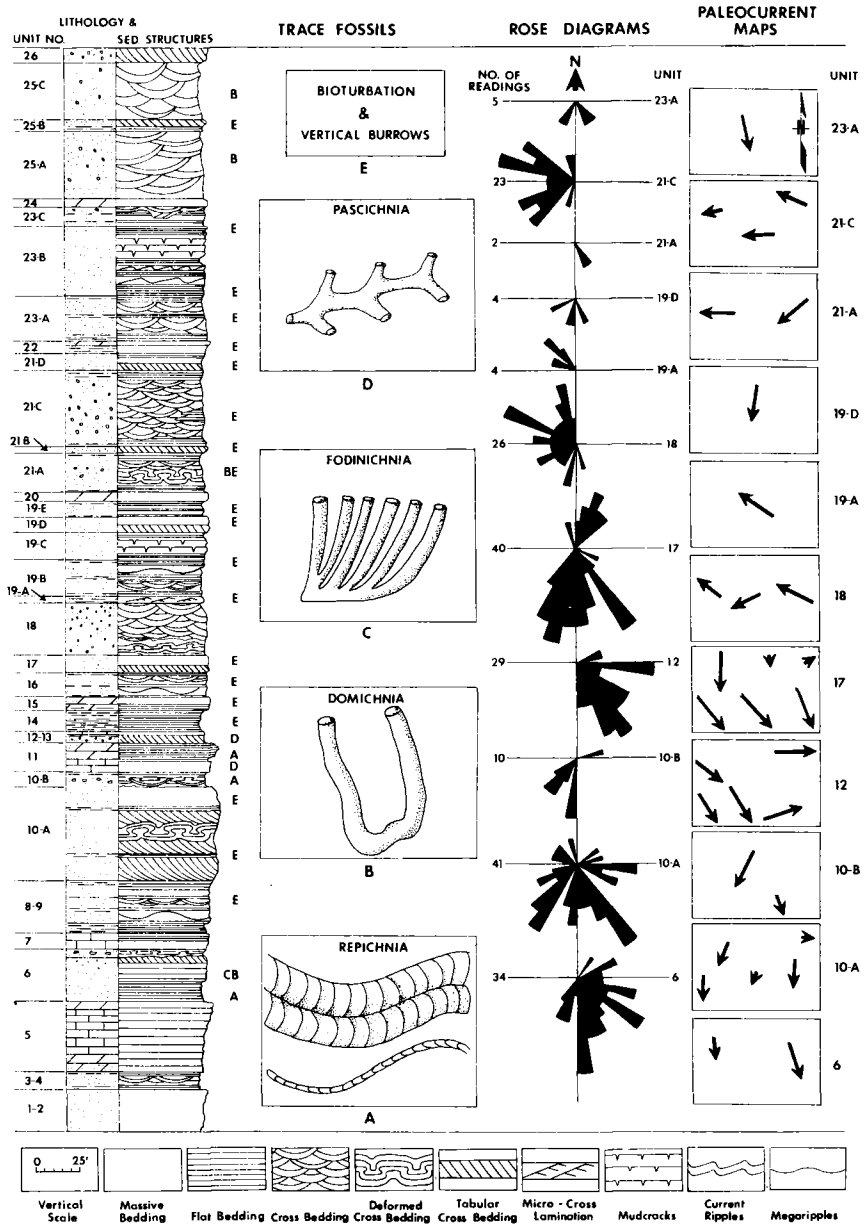
STRATIGRAPHIC SUBDIVISIONS

Rocks in the study locale are interbedded red beds and carbonates. They are subdivided into numerical units on the basis of color, lithology, and weathering characteristics. They are further subdivided into alphabetical subunits based on lithologies, sedimentary structures, and fossil content.

CLASTIC ROCKS

Clastic deposits in the principal section (Text-fig. 3) include coarse-grained purple arkose, coarse-grained white or light gray arkose, fine-grained purple arkose, fine-grained orange and white sandstone, very fine-grained silty orange sandstone, and silty maroon-and-gray shale. Sedimentary structures present include current and oscillation ripple marks, megaripple marks, mudcracks, trough cross-bedding, tabular cross-bedding, cusped ripple marks, flat bedding, contorted bedding, and intraformational conglomerates.

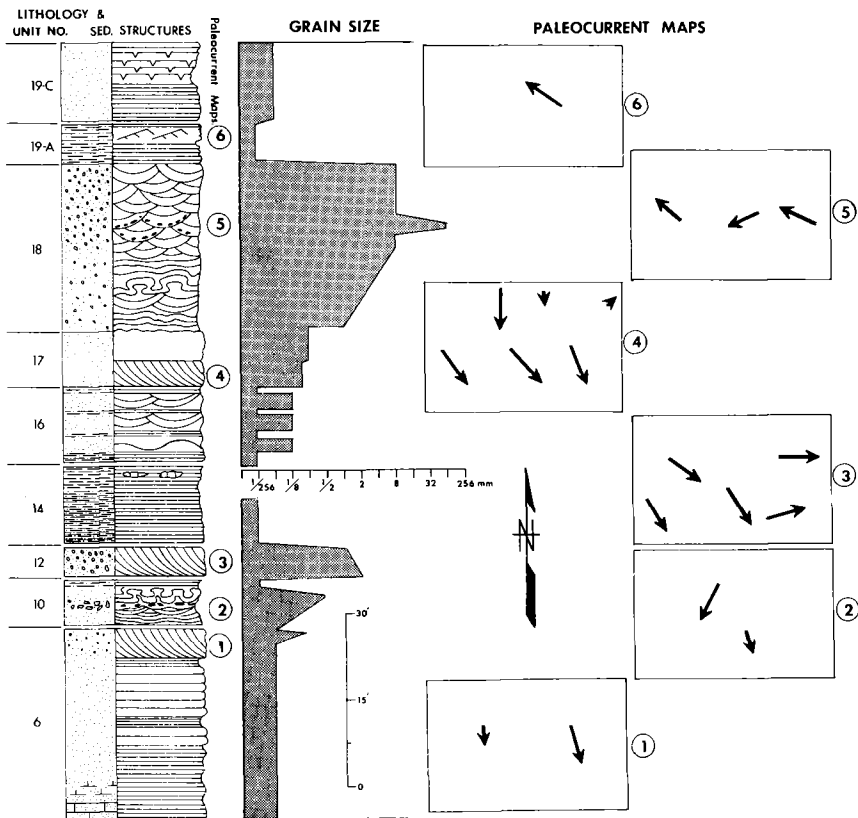
Coarse-grained purple arkose occurs in units 21-C, 25-A, 25-C, at the top of unit 21-A, and at the middle and top of unit 18 (Text-fig. 3). These units represent the coarsest and most immature deposits in the principal section. Large grain size, poor sorting, abundant feldspars, and rock fragments are typical of these units. Grain size ranges from medium-grained sand to coarse-pebble gravel (Text-fig. 4). Grain size generally appears to increase upwards within each of these deposits. Coarse-grained purple arkose deposits are made of trough cross-bedded sets 8 inches high and 30 to 60 inches long (Pl. 2, fig. 9). The coarsest clastic particles are found at the bases of individual cross-beds. Small and large lenses of very fine-grained purple arkose, *deformed cross-bedding, and flame structures are occasionally found here.* The paleocurrent for coarse-grained purple arkose units tends toward the west. However, numerous southwesterly and northwesterly current directions were obtained (Text-figs. 3, 4). Unit 21-A appears to have an anomalous paleocurrent trend, probably because of an insufficient number of



TEXT-FIGURE 3.—Total studied stratigraphic section, showing lithology and sedimentary structures. Trace fossils, Paleocurrent rose diagrams, and vector maps are keyed to stratigraphic sections. Arrows on vector maps represent clusters of paleocurrent direction readings and are spatially placed. Vector length indicates general tendency of paleocurrent direction. Note general paleocurrent direction to south and west.

measurements. Basal contacts of the coarse-grained purple arkose units are depositional or erosional surfaces (Pl. 2, fig. 6).

Coarse-grained white arkose occurs in units 12 and 26 and in the bottom of unit 16 (Text-figs. 3, 4). These rocks are similar in composition and texture to the coarse-grained purple arkose, except for abundant calcite cement. Large tabular cross-bedding, with sets generally two to four feet high and four to six feet long (Pl. 2, fig. 4), make up the deposits. Unit 12 thins and pinches out to the south in the principal and auxiliary reference



TEXT-FIGURE 4.—Stratigraphic column of selected clastic units, showing variations in lithology, sedimentary structures, grain size, and paleocurrent direction. Arrows on vector maps represent clusters of paleocurrent direction readings and are spatially placed. Vector length indicates general tendency of paleocurrent direction. Note diversity of lithologies and sedimentary structures, and increase in grain size upwards in the studied section. Unit 6 is a barrier-bar sequence. Its basal half is a fore-bar deposit and transition sequence from open-marine to clastic-dominated environment. Unit 10 is a delta-front deposit. Unit 12 is a very coarse-grained barrier-bar deposit. Unit 14 is an interdistributary-bay deposit. Unit 16 is a tidal-channel deposit. Unit 17 is delta material reworked into barrier or eolian-sand-bar deposit. Unit 18 is a channel or fluvial deposit. Unit 19-A is an arkosic micro-cross-laminated siltstone associated with channel deposits. Unit 19-C is a tidal-flat deposit.

sections. Paleocurrent data (Text-figs. 3, 4) indicates a southerly and southeasterly trend of the depositing current of unit 12.

Fine-grained purple arkose is abundant in the studied area and occurs in unit 4, at the top of 6, in 9, 10-B, and 16, at the bottom of 18, and in 19-A, 21-A, 23-C, and 25-C. It ranges from arkosic salt-and-pepper-like sandstone to silty, fine-grained purple arkose. Immaturity and bimodal size distribution are evident features of the fine-grained purple arkose (Pl. 3, figs. 2, 3, and 4). Grain size ranges from silty, fine-grained sand to medium-grained sand (Text-fig. 4). An example of floating grain texture can be seen at the base of unit 18 where the white calcite matrix isolates individual grains from one another. Generally, fine-grained purple arkose units underlie and overlie fine-grained orange sandstone units. Carbonate units in the lower part of the studied section consistently overlie fine-grained purple arkose, whereas in the upper part of the studied section, carbonate units are overlain by fine-grained purple arkose (Text-fig. 3). Fine-grained purple arkose also occurs under and interbedded with the coarse-grained purple arkose units.

Sedimentary structures are varied in the fine-grained purple arkose rocks (Text-figs. 3, 4) and include thin, flat bedding, small-scale trough cross-bedding, deformed and contorted bedding (Pl. 2, fig. 2), micro-cross-laminations, megariipple marks (Pl. 2, fig. 8), and intraformational conglomerates. Flat bedding and trace fossils are the most common features of this lithology. Paleocurrent data for this rock type vary, showing an erratic southerly and westerly trend.

Fine-grained orange and white sandstone occurs in units 6, 10-A, 17, 19-D, 21-B, and 21-D and is made up predominantly of clean quartz sand with 1 to 10 percent mica. Some units contain large amounts of calcite cement, producing floating grain textures such as are seen in the base of unit 17. Grain size is generally very fine-grained sand with some bimodal size distribution in units 6 and 17. Grain size in white sandstones ranges from fine-grained sand at their bases to medium-grained sand at their tops. The degree of sorting and rounding displayed in these units generally indicates a higher degree of maturity than that of other clastic deposits of the studied section. Deposits are usually thin bedded at their base, medium bedded in the middle, and tabular cross-bedded on top. Granule- and pebble-size grains are scattered in the tabular cross-bedded portion of these deposits. Fine-grained orange and white sandstone contains large-scale tabular cross-bedding which varies in height from six inches to five feet and in length from two to several feet (Pl. 2, figs. 1, 7). Paleocurrent data for fine-grained orange sandstones show a strong southwesterly trend which is commonly bimodal, whereas the white sandstones show a southeasterly trend. One fine-grained orange sandstone can be seen in unit 17 exhibiting geometry typical of a current-directed marine sand body. The bottom half of the sandstone body has a paleocurrent direction to the southwest. Its upcurrent end is thicker, and its upper half has a paleocurrent direction to the north. Tabular cross-bedding in fine-grained orange sandstone is generally overlain by bioturbated massive sandstone of the same lithology.

Very fine grained silty orange sandstone occurs in units 19-C and 23-B. It is generally composed of quartz sand with minor amounts of silt, clay chips, and mica. Mudcracks are the most common sedimentary structures.

Current and oscillation ripple marks, cusped ripple marks, and tabular cross-bedding are also present.

Maroon and gray silty shale occurs in units 8 and 14. Clay chips and mica are the only accessory grains. No sedimentary structures except flat bedding can be observed in either unit.

CARBONATE ROCKS

There are seven major carbonate units in the principal section, and they comprise just less than 100 feet of the total thickness, with individual carbonate units thinning towards the top of the section. The lowest studied

EXPLANATION OF PLATE 1

FIELD VIEWS

- FIG. 1.—View of principal section looking south across U.S. Highway 160. Carbonate marine deposits dominate in lower half of the section. Clastic deposits dominate in the upper half of the section.
- FIG. 2.—Top of unit 14 and bottom of unit 15. *Chonetes* zone at bottom of photo is overlain by maroon and gray silty shale containing *Linoproductus*, *Euphemites*, *Pharkidonotus*, and *Nuculana*. Unit 15 is probably a near-shore carbonate deposit which is bioturbated and contains *Linoproductus*, *Oriculoidea*, and crinoid debris. Tape in center of photo. Scale in lower right corner.
- FIG. 3.—Units 1 through 6. Massive quartz sandstone at bottom. Calamitian stem found here. Directly above is fine-grained purple arkose, overlain by thickest limestone unit in principal section, which is dolomitic near the base. From bottom to top, limestone contains bryozoans, crinoid debris, brachiopods, corals and echinoid spines. Succession of organisms is probably environmentally controlled. *Syringopora* is found at top of first ledge between units 5 and 6. Caninid corals are found 5 to 10 feet below the bottom of unit 6. Base of unit 6 is a highly bioturbated dolomitic quartz sandstone which coarsens upwards to medium-size quartz sandstone with horizons of domichnia descending several feet into finer dolomitic sand. Repichnia are also abundant near top. Burrowed sequence is capped by large tabular cross-beds of fine- to medium-grained sandstone with scattered grit-size pebbles. Paleocurrent directions trend to the southeast. Note man in lower right corner for scale.
- FIG. 4.—Units 15-26. Clastic and dolomitic deposits of upper half of principal section. Units 15 through 20 (extreme lower left corner to thin ledge on slope in mid-photo) exemplify a delta-complex cycle. Delta-complex cycles are usually bounded by limestones or ledge-forming dolomites. Sequence from base is lagoon, tidal channel, barrier bar, distributary channel, tidal channel, tidal flat, barrier bar, and lagoon.
- FIG. 5.—Unit 20. A biohermal dolomite in auxiliary reference section. Hammer in upper middle of photo is scale.
- FIG. 6.—Units 11-A through E. The richest fossil-bearing deposits in the studied section. Massive limestone in top of photo is coral unit. Repetitive ledges and slopes contain brachiopod assemblage. In bottom ledge, thin layer of fusulinid coquina is present. Scale lower right corner.
- FIG. 7.—Typical ledge-forming dolomite in clastic deposits. Contains ghosts of *Straparollus* and *Wilkingia*. This type of deposit is usually underlain by bioturbated orange sandstone and overlain by bioturbated fine-grained purple arkose.



1



2



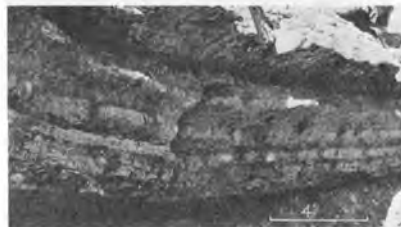
3



4



5



6



7

PLATE 1



1



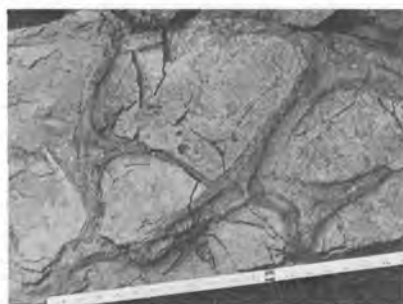
2



3



4



5



6



7



9



8

carbonate unit is 40 feet thick, whereas the uppermost one is less than 2 feet thick. Lowermost carbonate units are complex, formed of many lithologies, whereas uppermost ones are simple and usually are of one lithology, generally sparry dolomite.

The succession of lithologies in unit 11 represents a typical and nearly complete sequence of carbonate deposition, as is seen within the principal section. Other carbonate units in the section appear to be variations of this sequence (See appendix for detailed descriptions of carbonate units). The upper part of the sequence is high-energy deposits of dolomitic quartz sandstone that grades downward through sparry dolomite into an algal dolomite (units 11-G and F). Rocks in the upper middle part of the sequence are slightly argillaceous micritic limestone (Pl. 4, fig. 3) containing a moderate amount of skeletal debris (unit 11-E). Clay content and skeletal debris are more abundant in the lower part of the sequence (units 11-C and D). However, deposits here may or may not contain lithoclastic material (Pl. 4, fig. 4). The bottom of the sequence is argillaceous, skeletal, micritic limestone which has been diagenetically dolomitized (units 11-A and B). Included in this part are large areas where dark-colored carbonate clasts float in a lighter-colored matrix (unit 11-B) which may be evidence of a solution or a limited part of the above-described sequence. The base of unit 6 is

EXPLANATION OF PLATE 2

FIELD VIEWS OF ROCK UNITS

- FIG. 1.—A barrier or marine bar deposit. Upper portion of unit 6. Tabular cross-bedded rocks. Paleocurrent direction is to the southeast. This unit is a clean quartz sandstone with occasional grit-size grains. It is underlain by bioturbated sandstone and capped by fine-grained purple arkose similar to that of Figure 2 of Plate 2. Tape in mid-photo is scale.
- FIG. 3.—Unit 10-A. Large blowout deformation in fine-grained tabular cross-bedded, orange sandstone. This is possibly an eolian deposit. Scale in lower right corner.
- FIG. 4.—Unit 12. A storm-deposited barrier bar washover fan. Tabular cross-bedding in coarse-grained white arkose. Overlies and grades into dolomitic sandstone of unit 11-G. Capped by silty shale of unit 14 and limestone of unit 13. Paleocurrent direction is southeasterly.
- FIG. 5.—Unit 19-C. Tidal-flat deposit. Mudcracks and bioturbation in very fine-grained orange sandstone.
- FIG. 6.—Unit 18. A delta-front deposit. Contact between coarse- and fine-grained purple arkoses. Upper arkose is very coarse grained with abundant trough cross-bedding and represents a channel deposit. Lower arkose is bioturbated, fine-grained, and deformed.
- FIG. 7.—Unit 10-A. Bar deposit. Probable reworked delta sediments. Tabular cross-bedding in fine-grained orange sandstone. Paleocurrent direction is southwest. Note burrows immediately above cross-bedding. Scale in lower right corner.
- FIG. 8.—Unit 9. Tidal-channel deposits. Megaripples and interbedded fine-grained purple arkose and siltstone. Clipboard in center of photo is in megaripple trough. Scale in lower right corner.
- FIG. 9.—Unit 18. Trough cross-bedding in distributary-channel deposit. Paleocurrent direction is westerly.

breccia or an algal limestone. A thin fusulinid limestone is generally present at the very base of the unit (Pl. 4, fig. 2) and rests on a thin bed of calcareous green and blue gray silty claystone (top two inches of unit 10-B).

Unit 5 within the principal section contains basically the same succession of lithologies as is described in unit 11, except that it is three times thicker than unit 11. Other carbonate units appear to be made up of a single lithology analogous to unit 11-G. Unit 7, on the other hand, is the least argillaceous and most atypical carbonate unit. It is dark-colored micritic limestone with a strong petroliferous odor and contains sparsely scattered skeletal debris. The upper portion of unit 7 is a thin-bedded limestone of probable algal origin and contains patches of a possible solution breccia and an intraformational conglomerate.

Unit 13 is a light-colored, skeletal micritic limestone. It is the most argillaceous and least dolomitic carbonate unit in the principal section.

Units 15, 20, 22, and 24 are sparry dolomite, containing crystallized carbonate fossil ghosts and varying amounts of lithoclastic material. Units 20 and 24 contain isolated biohermal patches (Pl. 1, fig. 5). A four-inch dolomite layer, probably of algal origin (Pl. 2, fig. 8), is interbedded with the clastics of unit 9.

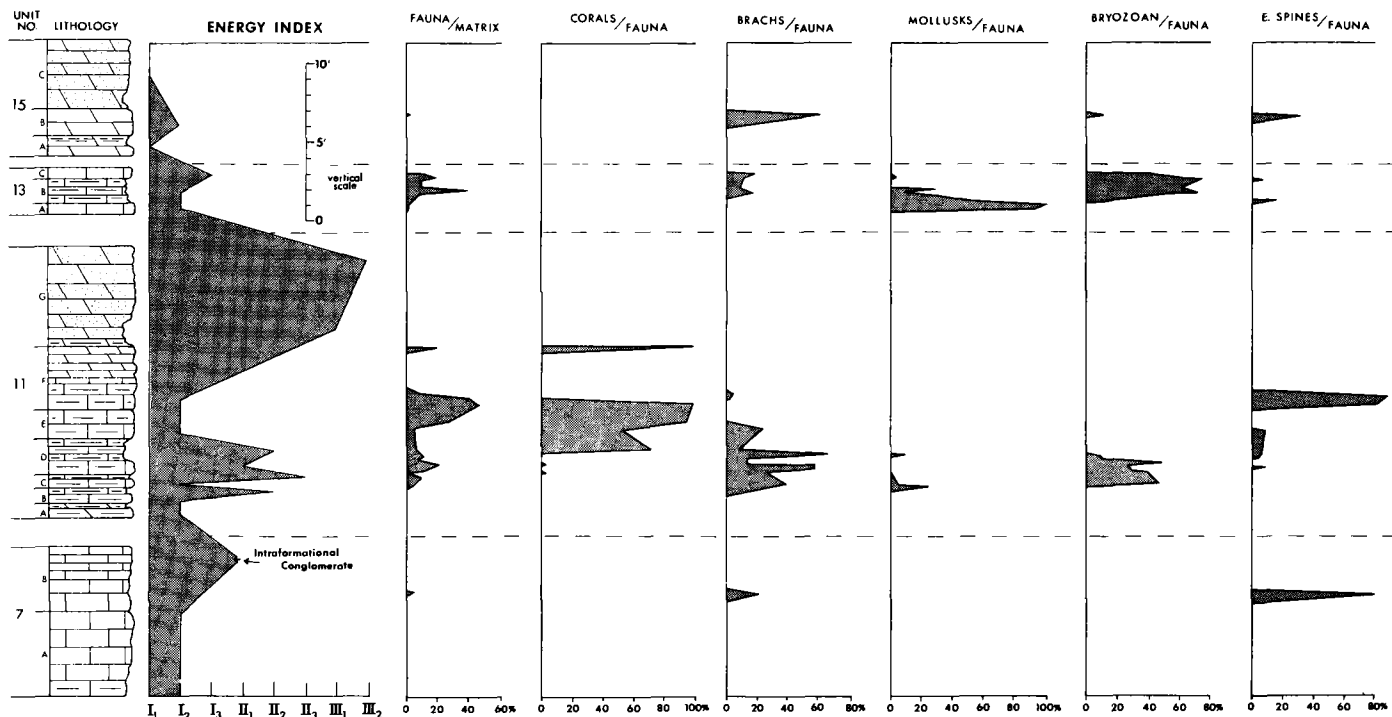
Light green and gray clays are present in most carbonate units and are generally found on bedding-plane surfaces. The green clay is probably glauconitic. Units 5, 11, and 13 show layers which weather into thin, wavy, ledge-like beds and undercut slopes (Pl. 1, fig. 3). Weathering habit is greatly influenced by mode of deposition and clay content of the rocks.

Plumley et al. (1962) developed the energy-index concept to show degree of water agitation near or at the depositional interface between water and sea floor. Physical parameters used for energy classification in the present study (Text-fig. 5) are size, sorting, roundness of granular particles, and nature of matrix. Secondary considerations are mineralogy and types and abundance of fossils. Five major degrees of water agitation are recognized, each with three subdivisions. Type I is a quiet-water limestone. Type II is intermittently agitated-water limestone, and Type III is slightly agitated-water limestone. Type IV is moderately agitated-water limestone, and Type V is strongly agitated-water limestone.

Overall water energy was not high during deposition of the carbonate units. It ranges from the very low energy of a quiet-water environment to the moderate energy of a slightly agitated-water environment. Carbonate units generally show evidence of higher-energy deposits at their bases and tops, and lower-energy deposits in mid-unit. Deposits of higher-energy environments form at least two-thirds of the carbonate rock thicknesses. Fossils are generally found in rocks of the lowest energy environments, brachiopods being the exception. The environments of unit 11-G increased in energy with the change from the carbonate environment of unit 11 to the clastic environment of unit 12 (Text-fig. 5).

INVERTEBRATE FOSSILS

Invertebrate fossils are almost exclusively restricted to carbonate rocks (units 5, 7, 11, 15, 22, and 24). An exception is unit 14, a silty maroon-and-gray shale. Approximately 80 feet of the 600-foot section contain invertebrate fossils.



TEXT-FIGURE 5.—Selected carbonate units, showing percentage of total fauna compared to matrix and percentage of selected fauna compared to total fauna. Energy Index after Plumley et al. (1962). I₁, I₂, and I₃: Deposition in quiet water; II₁, II₂, and II₃: Deposition in intermittently agitated water; III₁, and III₂: Deposition in slightly agitated water. Quiet environments generally contain more fauna than agitated environments. Note low diversity of coral-occupied environments. Unit 7 is an intertidal and/or supratidal environment. Unit 11 is a typical nonmarine deposit. Unit 13 is a carbonate-mud lagoon deposit. Unit 15 is a near shore environment.

Density of invertebrate fossils is as high as 50 percent of the rock body in portions of units 11 and 13; but in other units (5, 7, 14, 15, 22, and 24), fossils occupy 1 percent or less of the rock volume (Text-fig. 5). Diversity within the invertebrate-fossil-bearing rock is high. On the generic and specific levels there are more than 50 kinds of organisms (Table 1). A more exhaustive study could double that number.

The main invertebrate phyla are shown in Text-figure 5. The column labeled Fauna/Matrix shows in percentages the space occupied by the total faunal population as compared to rock matrix. The other columns show in percentages the space occupied by each phylum as compared to that occupied by the total fauna. Text-figure 6 shows the same data on a generic level.

EXPLANATION OF PLATE 3

PHOTOMICROGRAPHS OF CLASTIC ROCKS

- FIG. 1.—Unit 18. Typical coarse-grained purple arkose, 6x.
 FIG. 2.—Unit 18. Typical fine-grained purple arkose, 6x.
 FIG. 3.—Unit 12. Typical bimodal sandstone, 6x.
 FIG. 4.—Unit 16. Micro-cross-laminations, 6x. Very silty sandstone. Long, dark particles are mud chips.

EXPLANATION OF PLATE 4

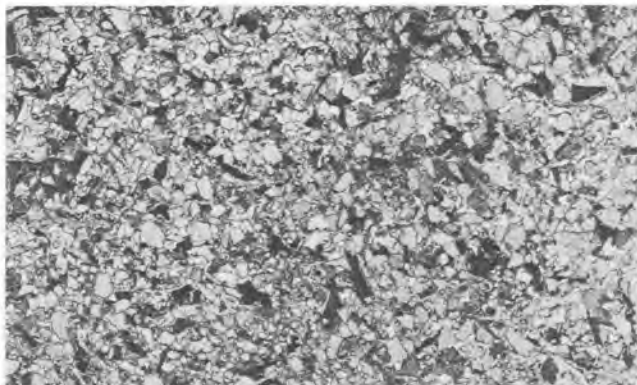
PHOTOMICROGRAPHS OF LIMESTONES

- FIG. 1.—Skeletal limestone, 6x.
 FIG. 2.—Bottom of Unit 11-A. Fusulinid limestone, 6x. Diagenesis prohibited positive identification.
 FIG. 3.—Unit 11-B. Skeletal micritic limestone, showing bryozoan and crinoid debris, 6x.
 FIG. 4.—Unit 11-D. Lithoclastic skeletal micritic limestone, 6x. Note abundance of quartz.

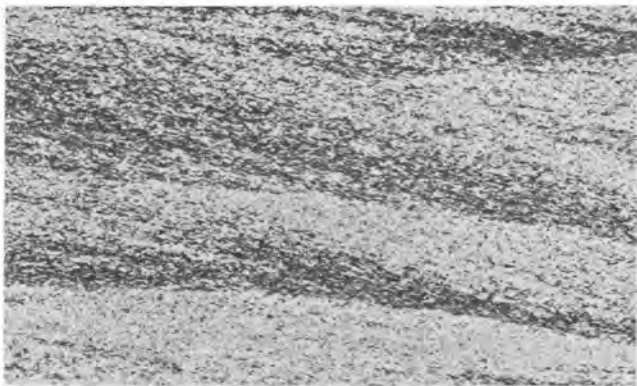
EXPLANATION OF PLATE 5

CORALS, GASTROPODS, AND OTHER FOSSILS

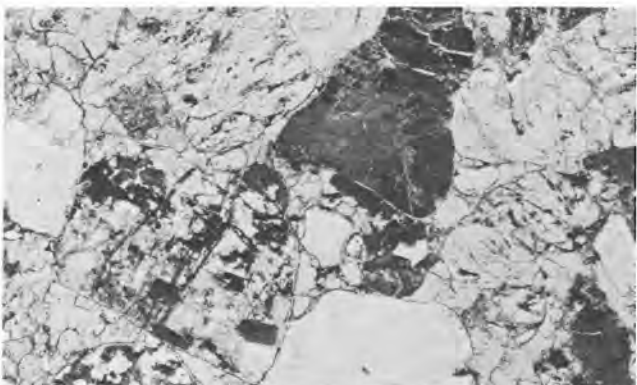
- FIG. 1.—*Caninia torquia* (Owen), side view, $\frac{3}{4}$ x, BYU 2003.
 FIG. 2.—Unit 11-E. *Euphemites* sp., dorsal view, 1x, BYU 2004.
 FIG. 3.—Top of Unit 13. *Bellerophon* sp., apertural view, 1x, BYU 2005.
 FIG. 4.—Unit 11-E. *Lophopyllidium profundum* (Edwards and Haime), side view, 1x, BYU 2006.
 FIG. 5.—Unit 13. *Euphemites carbonarius* (Cox), apertural view, 1x, BYU 2007.
 FIG. 6.—Unit 14. *Pharkidonotus percarinatus* (Conrad), dorsal view, 1x, BYU 2008.
 FIG. 7.—*Knighites montfortianus* (Norwood and Pratten), dorsal view, 1x, BYU 2009.
 FIG. 8.—Unit 11-F. *Syringopora* sp., side view, $\frac{1}{2}$ x, BYU 2010.
 FIG. 9.—Unit 11-D. *Ditomopyge* sp., dorsal view of pygidium, 1x, BYU 2011.
 FIG. 10.—Unit 11-D. Demosponge, top view, 1x, BYU 2012.
 FIG. 11.—Unit 14. *Anomphalus rotulus* (Meek and Worthen), apical view, 1x, BYU 2013.
 FIG. 12 and 15.—Unit 11-D. *Delocrinus*, ventral and dorsal views, 1x, BYU 2014 and 2040.
 FIG. 13.—Top of Unit 13. Crinoidal limestone, approx. $\frac{3}{4}$ x, BYU 2048.
 FIG. 14.—Unit 11. Bryozoan cluster, approx. $\frac{1}{2}$ x, BYU 2049.
 FIG. 16.—Unit 11-E. Coral layer (scale: steel tape).
 FIG. 17.—Unit 11-G. Coral cluster in living position (scale: pencil).



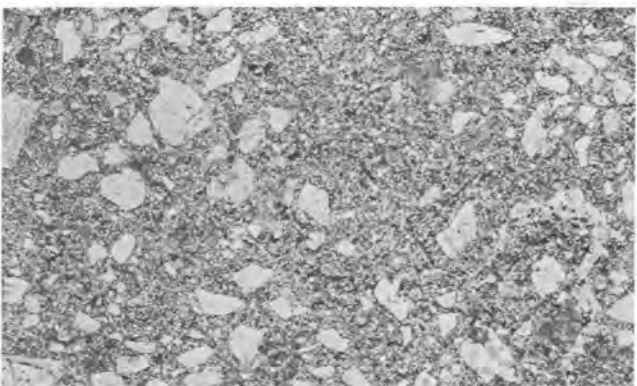
2



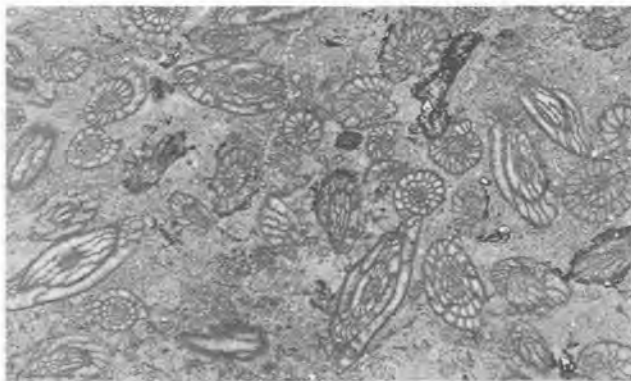
4



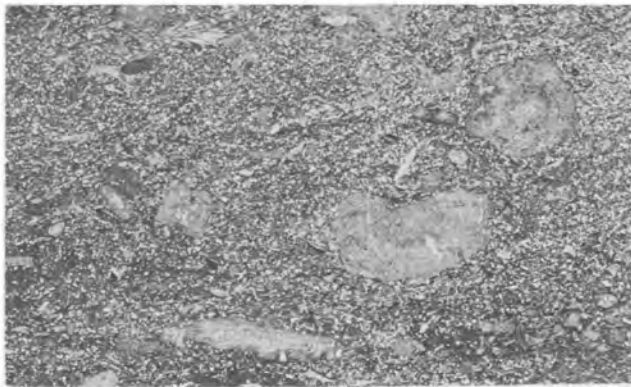
1



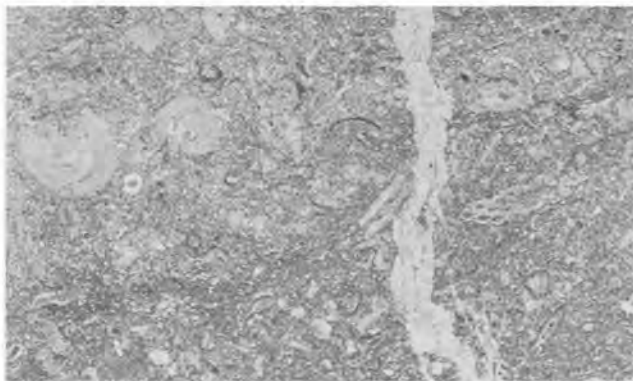
3



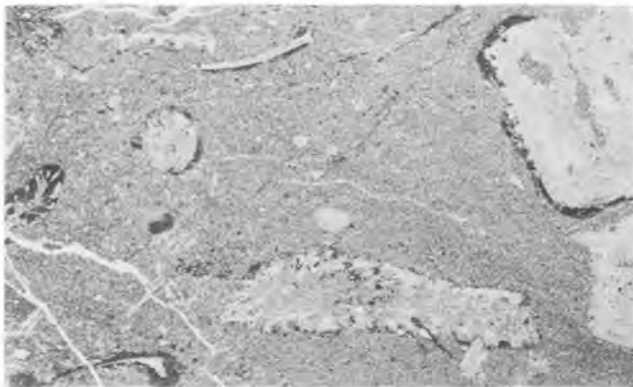
2



4



1



3

PLATE 4



PLATE 5

TABLE 1
Distribution of Fossil Species in Studied Section

FOSSILS	UNIT															
	5	7A	7B	11A	11B	11C	11D	11E	11F	13A	13B	13C	14	15	20	
Corals																
<i>Caninia torquia</i>	X	--	--	--	--	X	X	X	--	--	--	--	--	--	--	--
<i>Lophophyllidium profundum</i>	X	--	--	--	--	X	X	X	--	--	--	--	--	--	--	--
<i>Syringopora</i>	X	--	--	--	--	--	X	X	--	--	--	--	--	--	--	X
Biachiopods																
<i>Chonetes granulifer</i>	--	--	--	--	--	X	X	X	--	--	X	X	X	--	--	--
<i>Chonetina flemingi</i>	--	--	--	--	--	--	--	--	--	--	X	--	X	--	--	--
<i>Composita</i>	--	X	--	--	--	X	X	--	--	--	--	--	--	--	--	--
<i>Composita subtilita</i>	X	X	--	X	X	X	X	X	--	X	X	--	--	--	--	--
<i>Derbyia?</i>	--	--	--	--	--	--	X	X	--	--	--	--	--	--	--	--
<i>Derbyia bennetti</i>	--	--	--	--	--	--	X	X	--	--	X	--	--	--	--	--
<i>Derbyia crassa</i>	--	--	--	--	--	--	X	X	--	--	--	--	--	--	--	--
<i>Derbyia wabashensis</i>	--	--	--	--	--	--	X	--	--	--	--	--	--	--	--	--
<i>Dictyoelostus americanus</i>	--	--	--	X	--	X	X	X	--	--	--	--	--	--	--	--
<i>Echinoconchus?</i>	--	X	--	--	--	--	--	--	--	--	--	--	--	--	--	--
<i>Echinoconchus semipunctatus</i>	X	--	--	--	--	--	X	X	X	X	--	--	--	--	--	--
<i>Juresania nebrascensis</i>	--	--	--	--	--	--	X	X	--	--	X	X	--	--	--	--
<i>Linoproductus?</i>	--	X	--	--	--	--	--	--	--	--	--	--	--	--	--	--
<i>Linoproductus meniscus</i>	--	--	--	--	--	--	--	--	--	--	--	X	X	X	--	--
<i>Linoproductus prattenianus</i>	--	--	--	--	--	--	--	--	--	--	--	--	--	X	--	--
<i>Marginifera lasallensis</i>	--	--	--	--	X	X	X	--	--	--	X	X	--	--	--	--
<i>Marginifera wabashensis</i>	--	--	--	--	--	X	X	--	--	--	X	X	--	--	--	--
<i>Neospirifer kansasensis</i>	X	--	--	X	X	X	X	--	--	--	X	X	--	--	--	--
<i>Neospirifer triplicatus</i>	--	--	--	--	--	X	X	--	--	--	--	--	--	--	--	--
<i>Orbiculoidea</i>	--	--	--	--	--	--	--	--	--	--	--	--	--	--	--	X
<i>Phricodothyris perplexa</i>	--	--	--	--	--	X	X	--	--	--	--	--	--	--	--	--
<i>Punctospirifer kentuckyensis</i>	--	--	--	--	X	X	X	--	--	--	--	--	--	--	--	--
<i>Wellerella osagensis</i>	--	--	--	--	--	X	X	--	--	--	--	--	--	--	--	--
<i>Wellerella tetrahedra</i>	--	--	--	--	--	X	X	--	--	--	--	--	--	--	--	--
Pelecypods																
<i>Acanthopecten carboniferus</i>	--	--	--	--	--	--	--	--	--	--	X	X	--	--	--	--
<i>Aviculopecten</i>	--	--	--	--	--	--	--	--	--	--	X	X	X	--	--	--
<i>Chaenomya</i>	--	--	--	--	--	--	--	--	--	--	--	--	X	--	--	--
<i>Eimondia</i>	--	--	--	--	--	X	--	--	--	--	X	--	--	--	--	--
<i>Lima</i>	--	--	--	--	--	--	--	--	--	--	X	--	--	--	--	--
<i>Limapecten</i>	--	--	--	--	--	--	--	--	--	--	X	X	--	--	--	--
<i>Limatula</i>	--	--	--	--	--	--	--	--	--	--	X	X	--	--	--	--
<i>Myalina</i>	--	--	--	--	--	--	--	--	--	--	X	X	--	--	--	--
<i>Muculana bellistriata</i>	--	--	--	--	--	--	--	--	--	--	--	--	X	--	--	--
<i>Parallelodon</i>	--	--	--	--	--	--	--	--	--	--	--	--	X	--	--	--
<i>Permophorus occidentalis</i>	--	--	--	--	--	--	--	--	--	--	--	--	X	--	--	--
<i>Pseudomonotis</i>	--	X	--	--	--	--	--	--	--	--	--	--	--	--	--	--
<i>Pseudomonotis equistriata</i>	--	X	--	--	--	--	--	--	--	--	X	X	--	--	--	--
<i>Pseudomonotis kansasensis</i>	--	--	--	--	--	--	--	--	--	--	X	X	X	--	--	--
<i>Pteronites</i>	--	--	--	--	--	--	--	--	--	--	--	--	X	--	--	--
<i>Ptychomphalus</i>	--	--	--	--	--	--	--	--	--	--	--	--	--	X	--	--
<i>Schizodus</i>	--	--	--	--	X	--	--	--	--	--	X	X	--	--	--	--
<i>Septimyalina burmi?</i>	--	--	--	--	--	--	--	--	--	--	X	X	--	--	--	--
<i>Wilkingia</i>	--	--	--	--	X	X	--	--	--	X	--	--	--	--	--	--

Table 1 (Continued)

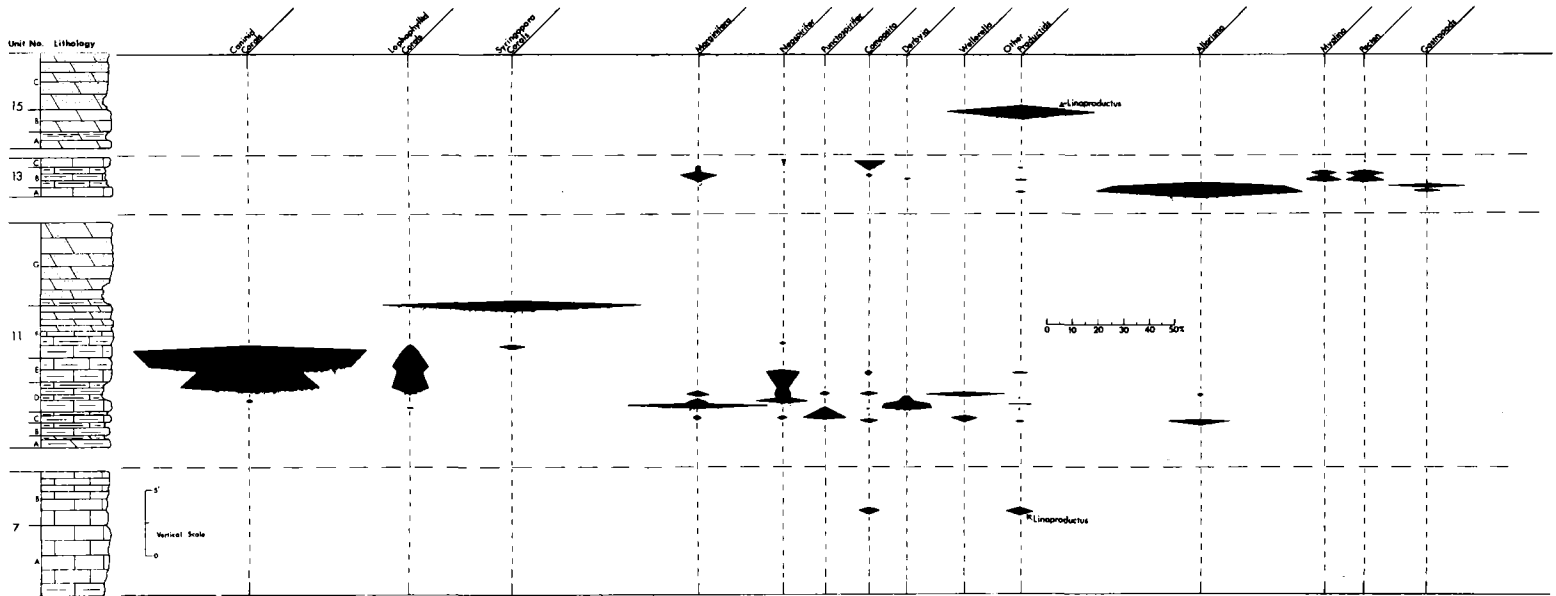
Gastropods															
<i>Anomphalus rotulus</i>	--	--	--	--	--	--	--	--	--	--	--	--	X	--	--
<i>Bellerophon</i>	--	--	--	--	--	--	X	--	--	X	X	--	X	--	--
<i>Bellerphontid</i>	--	--	--	--	--	--	--	--	--	--	X	--	--	--	--
<i>Euphemites carbonarius</i>	--	--	--	--	--	--	--	--	--	--	X	X	X	--	--
<i>Knightites montfortianus</i>	--	--	--	--	--	--	--	--	--	--	--	--	--	X	--
<i>Pharkidonotus percarinatus</i>	--	--	--	--	--	X	X	--	--	--	X	X	X	--	--
<i>Straparollus</i>	--	--	--	--	--	X	X	--	--	X	--	--	X	X	X
<i>Worthenia</i>	--	--	--	--	--	--	--	--	--	--	--	--	X	--	--
Miscellaneous															
Algae	X	--	X	--	--	--	--	--	X	--	--	--	--	--	X
Arthropod carapace	--	--	--	--	--	--	--	--	--	--	--	--	--	X	--
<i>Delocrinus</i>	--	--	--	--	--	--	X	--	--	--	--	--	--	--	--
Demospongea	--	--	--	--	X	X	--	--	--	--	--	--	--	--	--
<i>Ditomopyge</i>	--	--	--	--	--	X	X	--	--	--	--	X	X	--	--
<i>Echinocrinus</i>	X	X	X	--	X	X	X	X	--	--	--	X	--	X	--
Nautilus	--	--	--	--	X	--	--	--	--	--	--	--	--	--	--
<i>Triticites</i>	--	--	--	X	X	--	--	--	--	--	--	--	--	--	--
Bryozoans															
massive	X	--	--	--	--	--	X	X	--	--	--	--	--	--	--
massive branching	X	--	--	--	--	X	X	--	--	--	--	--	--	--	--
sheeting	X	--	--	--	X	--	--	--	--	--	X	X	X	X	--
twiggy branching	--	--	--	--	--	--	--	--	--	--	X	X	X	--	--

CORALS

Three coral forms are present: caninid, lophophyllid, and *Syringopora* (Text-fig. 6). Caninid corals are by far the most abundant and usually inhabit the least argillaceous, micritic limestone in the carbonate cycle. Corals are found in units 5, 11, and 22. They represent up to 99 percent of the fossils found in units 11-E, F, and G, indicating low fossil diversity and high fossil density (Text-figs. 5, 6). Plate 5, figure 16, shows in unit 11-F a layer in which caninid corals are extremely dense. An average specimen from this layer is illustrated in Plate 5, figure 1. Caninid corals within this dense layer are generally irregularly oriented, but a few are found upright. A small, *in situ* caninid coral cluster is found at the base of unit 11-G in the reference section (Pl. 5, fig. 17). It is an isolated circular cluster, 2.5 feet in diameter, containing mostly caninid corals, with minor numbers of lophophyllid corals. Bases of the corals are apparently attached to a limestone and are standing in tan, sandy, sparry dolomite of unit 11-G. Their spacing can best be seen in Plate 5, figure 17.

Lophophyllidium, the other prominent rugose coral found in units 5 and 11, is illustrated in Plate 5, figure 4. This small coral is not as abundant as caninid or *Syringopora* but usually is found in close contact with caninid corals and at the base of, or within, the *Syringopora* colonies. Lophophyllid corals are also found in small numbers in units 11-C and D (Text-fig. 6).

Syringopora is found most often in unit 11 (Text-fig. 6) but can also be found in units 5 and 22. One isolated example was found in unit 22 where fossils are usually scarce. At the contact between units 11-F and G, *Syringopora* is common. It is almost the only fossil present. In unit 11-F, isolated *Syringopora* heads are found surrounded by echinoid-spine debris.



TEXT-FIGURE 6.—Selected carbonate units, showing percentage of selected genera compared to total fauna. Note density of corals and diversity of brachiopods.

Corals are associated with particular fossils. The following fossil assemblage has been constructed from Table 1 and Text-figure 6:

Caninid corals	<i>Dictyoclostus</i> sp.
Lophophyllid corals	<i>Composita</i> sp.
<i>Syringopora</i> sp.	echinoid spines
<i>Neospirifer</i> sp.	crinoid debris
<i>Echinoconchus</i> sp.	

This fossil assemblage is generally found in dense, clean limestone like that of units 11-E and F.

BRACHIOPODS

Brachiopods are present in units 5, 7, 11, 13, 14, and 15. They appear in a variety of lithologies, ranging from the shale in unit 14 to the dense, clean limestone of unit 11-F. Brachiopods show greatest diversity in units 11-C and D (Text-fig. 6; Table I), an argillaceous, bioclastic, gray limestone (see midportion of Pl. 1, fig. 6). Fossil brachiopods are generally well preserved. Their shells are not usually abraded but are commonly crushed because of compaction. One *Neospirifer* from unit 11-C was partially crushed, but its spiral brachidia were left exposed and intact. Most brachiopods are of a relatively small size in areas such as those of unit 11-C and D, where diversity is great. Large *Derbyia bennetti* are exceptions.

The large productids *Echinoconchus* and *Dictyoclostus* (Pl. 7, figs. 6, 7, 11, 13) are principally confined to coralline facies (units 11-E and F) and to other areas of low diversity (units 11-A and B). In the lower halves of units 5 and 7, they are present in small numbers sharing the rock with echinoid spines, crinoid debris, and various kinds of bryozoans.

Linoproductus shares unit 15 with echinoid spines and crinoid debris and is commonly found resting on its pedicle valve in living position. *Linoproductus* (Pl. 7, figs. 5, 10) is also abundant along with *Chonetes* in unit 14.

Chonetes is found in small numbers in many units (Table I) but is abundant only in unit 14, where thin layers of densely packed, disarticulated valves lie parallel to one another (Pl. 6, figs. 7, 8, 9).

Neospirifer, *Composita*, and *Marginifera* are the most widely dispersed individuals and are found in varied lithologies. On the other hand, *Wellerella*, *Punctospirifer*, and *Phricodothyris* are restricted to units 11-C and D (Text-fig. 6).

In unit 11-C, *Marginifera* (Pl. 7, fig. 8; Pl. 6, fig. 24) occurs in small clusters of three to six specimens that seem to be attached to one another or to another brachiopod, usually *Neospirifer*. These clusters may represent the living positions of *Marginifera*. Approximately 10 percent of the fossils in unit 13 are *Marginifera* and/or *Juresania* (Text-fig. 6).

Composita is equally as abundant as *Marginifera* in unit 13, but not necessarily in the same layers. *Composita* can be found in living position, its brachial valve facing up and its anterior end protruding out of the limestone (units 11 and 13). Encrusting bryozoans are usually attached to the exposed portion of the shell.

Text-fig. 6 and Table 1 were used to construct the fossil assemblage for brachiopods that are common to lithologies like those of units 11-C and D. The assemblage is listed below:

<i>Echinoconchus</i> sp.	<i>Lophophyllidium</i> sp.	<i>Composita</i> sp.
<i>Wilkingia</i> sp.	<i>Ditomopyge</i> sp.	<i>Derbyia</i> sp.
<i>Myalina</i> sp.	crinoid debris	<i>Wellerella</i> sp.
<i>Bellerophon</i> sp.	<i>Marginifera</i> sp.	<i>Chonetes</i> sp.
<i>Pharkidonotus</i> sp.	<i>Neospirifer</i> sp.	<i>Dictyoclostus</i> sp.
<i>Straparollus</i> sp.	<i>Punctospirifer</i> sp.	<i>Phricodothyris</i> sp.

MOLLUSKS

Mollusks are present in units 11, 13, and 14, but are most abundant in units 13 and 14 (Table 1).

Wilkingia is the most abundant pelecypod (Text-fig. 6; Pl. 6, fig. 19) in units 11-B and C and unit 13-A, where it inhabits generally fossil-barren limestone. It can sometimes be found in red, crinoid-debris-filled trails. Other pelecypods are *Septimyalina* (Pl. 6, figs. 15, 18), *Acanthopecten* (Pl. 6, fig. 16), and *Lima* (Pl. 6, figs. 12, 14). These can be found in abundance in the upper portions of unit 13-B and C (Text-fig. 6).

Pelecypods are most abundant on bedding-plane surfaces in argillaceous limestones like those of unit 13. Below is the fossil assemblage found in unit 13. All of these organisms are generally found in close association on

EXPLANATION OF PLATE 6

BRACHIOPODS, BIVALVES AND BRYOZOANS

- FIGS. 1 and 2.—Unit 11-C and D. *Wellerella tetrahedra* (Dunbar and Condra), brachial and anterior views, 1x, BYU 2015.
- FIGS. 3 and 4.—Unit 11-C and D. *Wellerella osagensis* (Swallow), brachial and lateral views, 1x, BYU 2016.
- FIG. 5.—Unit 11-D. *Neospirifer* sp., brachial view, 1x, BYU 2047.
- FIG. 6.—Unit 11. *Phricodothyris perplexi* (McChesney), brachial view, 1x, BYU 2018.
- FIGS. 7, 8, and 9.—Units 11 and 14. *Chonetes granulifer* (Owen), dorsal (2) and anterior views, 1x, BYU 2019, 2042, and 2043.
- FIG. 10.—Unit 11-D. *Punctospirifer kentuckyensis* (Shumard), anterior view, 1x, BYU 2020.
- FIG. 11.—Units 11 and 13. *Composita subtilis* (Hall), brachial view, 1x, BYU 2021.
- FIG. 12.—Unit 13-B. *Limatula* sp., lateral view, 1x, BYU 2022.
- FIG. 13.—Unit 13. *Pseudomontis* sp., lateral view, 1x, BYU 2023.
- FIG. 14.—Unit 13-B. *Limapecten* sp., lateral view, 1x, BYU 2024.
- FIGS. 15 and 18.—Unit 13. *Septimyalina* sp., left and right valves, 1x, BYU 2025.
- FIG. 16.—Unit 13. *Acanthopecten carboniferous* (Stevens), right valve, 1x, BYU 2000.
- FIG. 17.—Unit 14. *Nuculana bellestriatia* (Stevens), left valve, 1x, BYU 2027.
- FIG. 19.—Unit 13. *Wilkingia* sp., left valve, approx. $\frac{2}{3}$ x, BYU 2023.
- FIG. 20.—Unit 13. *Wilkingia* sp., left valve, 1x, BYU 2041.
- FIG. 21.—Unit 11. *Neospirifer* sp., brachial view, 1x, BYU 2017.
- FIG. 22.—Unit 13. *Edmondia* sp., left valve, 1x, BYU 2002.
- FIG. 23.—Unit 14. *Parallelodon* sp., left valve, 1x, BYU 2029.
- FIG. 24.—Unit 13. Sheeting bryozoans, *Juresania* sp., and pelecypods, approx. $\frac{1}{2}$ x, BYU 2030.

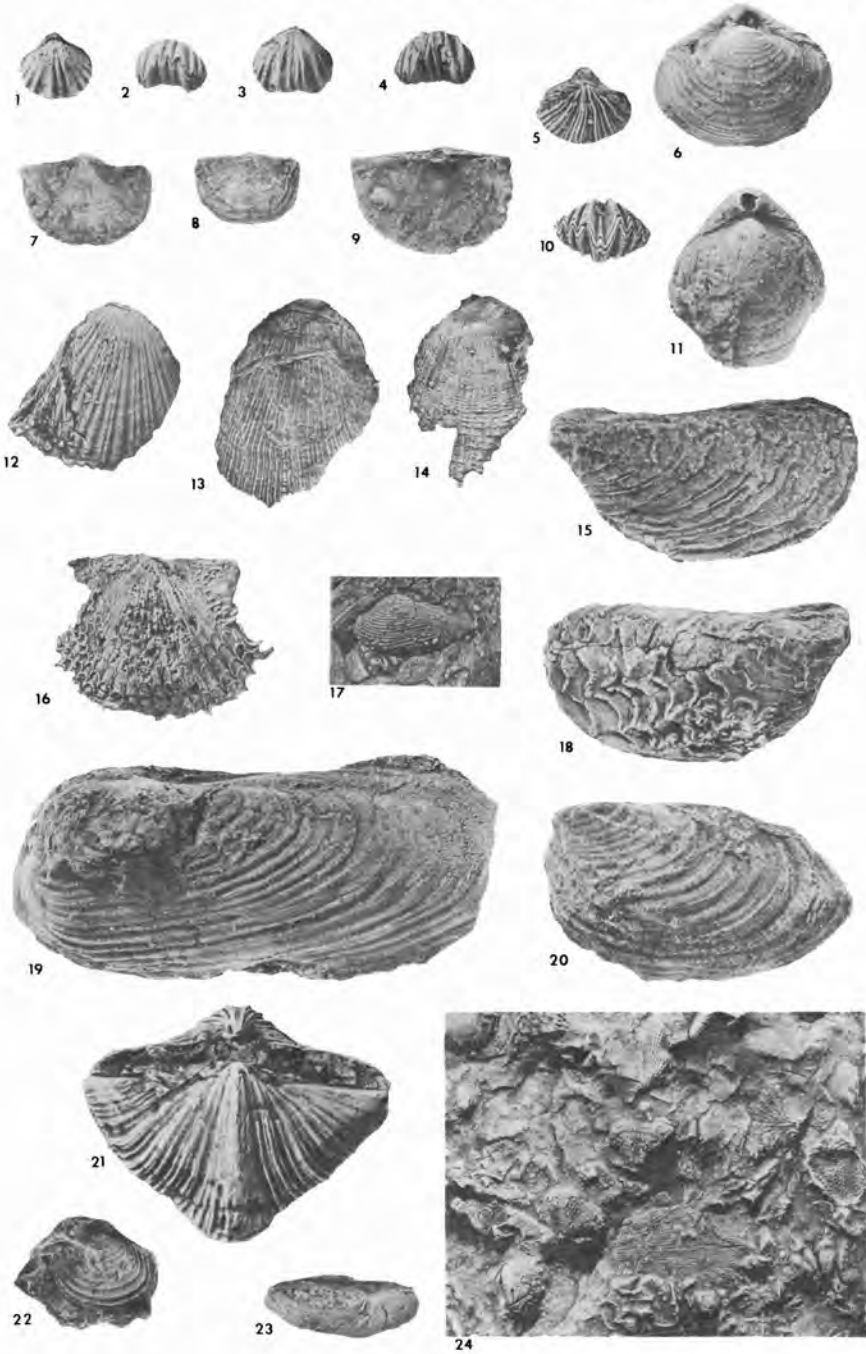


PLATE 6

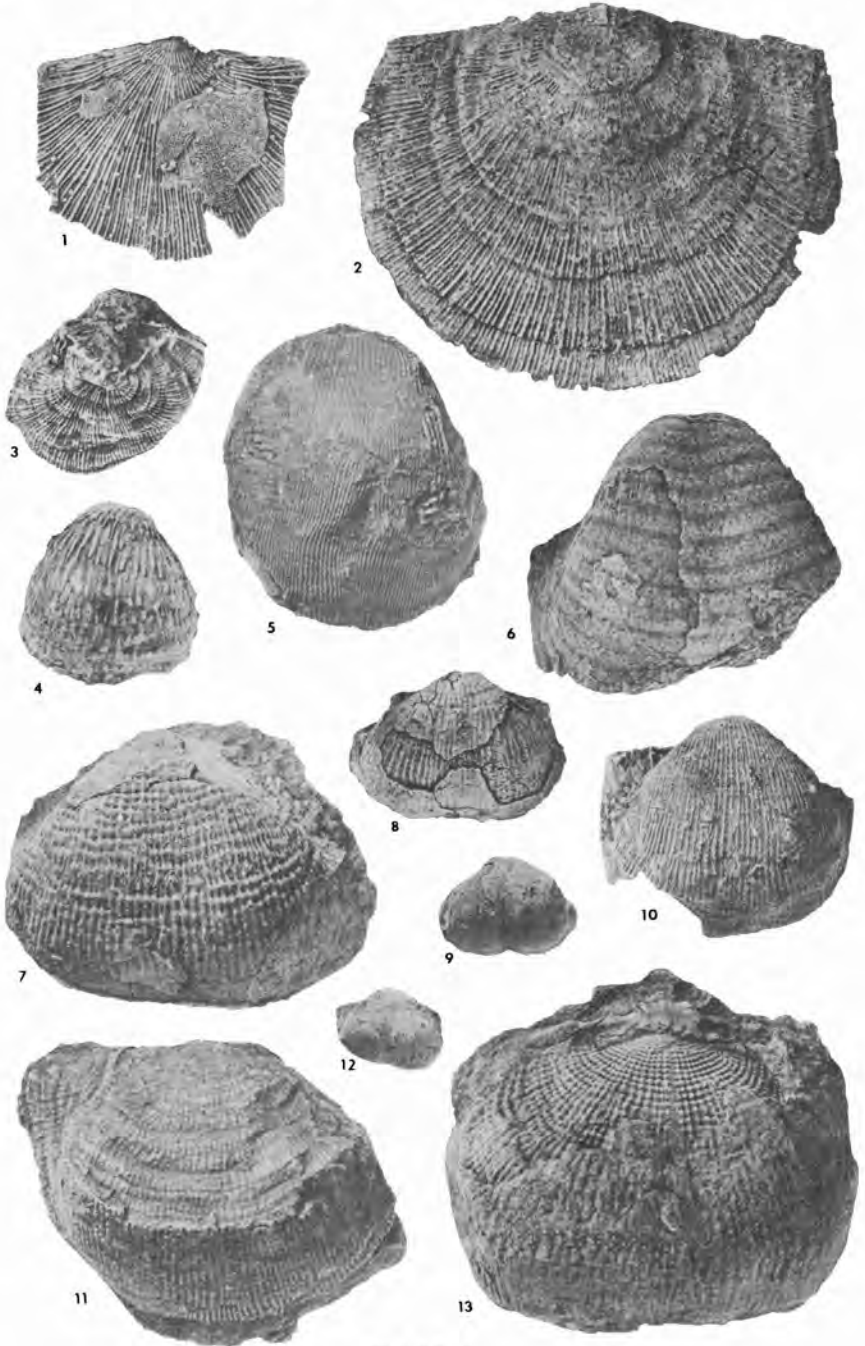


PLATE 7

bedding-plane surfaces and are usually covered with a mat of delicate, twiggy and sheeting bryozoans.

<i>Marginifera</i> sp.	<i>Myalina</i> sp.	<i>Straparollus</i> sp.
<i>Neospirifer</i> sp.	<i>Aviculopecten</i> sp.	<i>Bellerophon</i> sp.
<i>Composita</i> sp.	<i>Pecten</i> sp.	<i>Euphemites</i> sp.
<i>Derbyia</i> sp.	<i>Pseudomontis</i> sp.	<i>Ditomopyge</i> sp.
<i>Juresania</i> sp.	<i>Septimyalina</i> sp.	bryozoans
<i>Chonetes</i> sp.	<i>Acanthopecten</i> sp.	crinoid debris
<i>Wilkingia</i> sp.	<i>Lima</i> sp.	

Gastropods found in units 11-C and D are generally *Bellerophon* or *Straparollus* types, larger than similar genera in units 13 and 14. Gastropods and pelecypods are generally disseminated in the lower half of unit 14, a maroon-and-gray silty shale. Ordinarily, fossils are in upright positions and are not closely packed. *Pharkidonotus* (Pl. 5, fig. 6), *Knightites* (Pl. 5, fig. 7), *Euphemites*, and *Anomphalus* (Pl. 5, fig. 11) are abundant gastropods in unit 14. *Parallelodon* (Pl. 6, fig. 5), *Nuculana* (Pl. 6, fig. 17), and *Aviculopina* are among the abundant pelecypods found here. The fossil assemblage for unit 14 is listed below (from Table 1 and Text-fig. 6). These fossils are most abundant in shale.

<i>Chonetes</i> sp.	<i>Knightites</i> sp.	<i>Euphemites</i> , sp.
<i>Linoproductus</i> sp.	<i>Pleurophorus</i> sp.	<i>Chaenomya</i> sp.
<i>Straparollus</i> sp.	<i>Aviculopina</i> sp.	<i>Parallelodon</i> sp.
<i>Anomphalus</i> sp.	<i>Pharkidonotus</i> sp.	<i>Nuculana</i> sp.
<i>Ptychomphalus</i> sp.	<i>Bellerophon</i> sp.	

MISCELLANEOUS FOSSILS

Ditomopyge, the small trilobite, was found in units 11-C and 13-C. Only two pygidia were recovered (Pl. 5, fig. 9). Two demosponge specimens were recovered from unit 11-C (Pl. 5, fig. 10). Two crinoid calyces (Pl. 5, figs. 12, 15) were found in unit 11-C, although copious amounts of crinoid

EXPLANATION OF PLATE 7

BRACHIOPODS

- FIG. 1.—Unit 11-D. *Derbyia* sp., with encrusting bryozoans, posterior view, 1x, BYU 2026.
- FIG. 2.—Unit 11-D. *Derbyia* sp., brachial or dorsal view, 1x, BYU 2031.
- FIG. 3.—Unit 13. *Derbyia bennetti* (Hall and Clark), brachial view, 1x, BYU 2032.
- FIG. 4.—Unit 13. *Juresania nebraskensis* (Owen), brachial view, 1x, BYU 2033.
- FIG. 5.—Unit 14. *Linoproductus prattenianus* (Norwood and Pratten), pedicle, 1x, BYU 2034.
- FIG. 6.—Unit 11-D. *Echinoconchus* sp., dorsal view, 1x, BYU 2035.
- FIGS. 7, 11, and 13.—Units 7 and 11 *Dictyoclostus* sp., dorsal views, 1x, BYU 2001, 2036, and 2039.
- FIG. 8.—Unit 13. *Marginifera lasallensis* (Worthen), dorsal view, 1x, BYU 2046.
- FIGS. 9 and 12.—Unit 13. *Marginifera wabashensis* (Norwood and Pratten), dorsal views, 1x, BYU 2037, 2044, and 2045.
- FIG. 10.—Units 13, 14, and 15. *Linoproductus meniscus* (Dunbar and Condra), dorsal view, 1x, BYU 2038.

debris are found in units 5, 7, 11, 13, and 15 (Pl. 5, fig. 13). A fusulinid limestone is present at the contact between the base of unit 11 and the clastic unit below (Pl. 4, fig. 2). There is no apparent orientation to the fusulinids. Their positive identification has been prohibited by diagenetic alterations. They are also found in units 11-A and C. A straight nautiloid, approximately six inches long, was found in unit 11. A calamitian stem, found by Dr. W. D. Tidwell (personal communication, 1971), was the only plant remains found in the studied locale. It was recovered from the basal sandstone portion of unit 2 (Pl. 1, fig. 3). Biostromal dolomite and limestone are present in unit 11-F and at the top of unit 5. A dolomite that is biohermal in appearance is present in unit 22 (Pl. 1, fig. 5).

Bryozoans occur in units 5, 11, 13, and 14. They change form upward within units 11-C and D. In unit 11-C they are more delicate in form, appearing as sheeting and small, twiggy forms, while in unit 11-D they are massive branching forms, at least five times as large as those in unit 11-C. In unit 13 a few bedding-plane surfaces are matted with various kinds of sheeting and twiggy byozoans. These delicate forms appear to be un-abraded and certainly were not transported far.

SEQUENCE OF FOSSILS

In units 5 and 11 a general sequence of fossils is evident. Fusulinids occur at the base of unit 11 and are followed by byozoans and brachiopods. In the midsection of the unit, rugose corals dominate. These give way upward to algae and *Syringopora* (Text-fig. 6). As carbonate deposits grade upward to clastic deposits, various repichnid trace fossils appear.

Another sequence of fossils is seen in unit 13. *Wilkingia* is at the base followed in mid-unit mainly by pelecypods and brachiopods. These fossils are covered by a layer of delicate twiggy and sheeting bryozoans which in turn is covered by a red layer of densely packed crinoid debris (Text-fig. 6).

TRACE FOSSILS

Trace fossils are the most abundant fossils in the studied locale, and they provide keys for interpreting environments of deposition (Text-fig. 3). Trace fossils are classified according to Seilacher's (1964) terminology as *domichnia* (dwelling burrows), *fodinichnia*, (feeding burrows), *pascichnia* (feeding trails), *cubichnia* (resting trails), and *repichnia* (crawling trails). Distribution of trace fossils is plotted in Text-figure 3.

Domichnid burrows are found in units 6, 21-A, 25-A and 25-C. Most of these burrows found in unit 6 (Pl. 8, fig. 1) are one inch in diameter

EXPLANATION OF PLATE 8

TRACE FOSSILS

- FIGS. 1, 2, and 8.—Units 6, 25-A, and 26. Domichnia.
 FIGS. 3 and 5.—Unit 6. Repichnia.
 FIG. 4.—Unit 6. Fodinichnia.
 FIG. 6.—Unit 21-D. Bioturbation, pascichnia or repichnia.
 FIGS 7 and 9.—Units 13 and 11-E. Pascichnia.
 FIG. 10.—Unit 19-B. Vertical burrows.



1



2



3



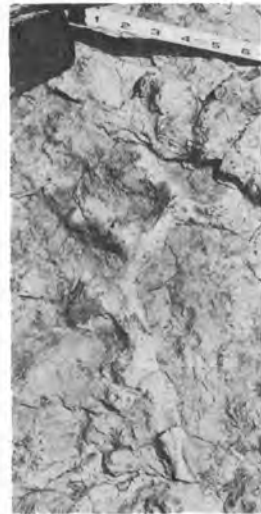
5



4



6



7



8



9



10

and are generally variable in length. However, near the top of unit 6, burrows are several feet long. The openings occur close together as pairs, indicating that the burrows are J- or U-shaped. Two burrowed layers, one foot to two feet thick, occur, one near the midsection and one near the top of unit 6 (Pl. 8, fig. 8). Here numerous burrows 0.75 inch in diameter and one foot to two feet long are imbedded in a dark-colored, finer-grained sandstone. These burrowed layers probably represent periods when sedimentation was slow and the biologic community had time to establish itself. Domichnid burrows in unit 6 are vertical, except for slight bends (Pl. 8, figs. 1, 8). Burrow fillings are generally finer grained, and darker green than the country rock.

An example of domichnid burrows as found in units 21-A, 25-A, and 25-C is shown in Plate 8, figure 2. These U- or J-shaped burrows of fine-grained, white, calcareous sandstone are imbedded in purple arkose. They are uncommon, occurring mostly in the upper parts of arkose units. They are three to four feet long and approximately two inches in diameter. They may be *Ophiomorpha* burrows but are too severely weathered for positive identification.

One example of fodinichnid burrows was recovered. The burrows are circular, 0.5 to 0.75 inch in diameter, and have rings or ridges on their walls (Pl. 8, fig. 4). They are similar to the illustration in Diagram C, Text-figure 3.

Pascichnid burrows are present only in the carbonate units (Pl. 8, figs. 7, 8, and 9). Pascichnid burrows in unit 11 are smooth walled, approximately three inches in diameter, and are darker colored and more siliceous than the country rock. Chert lenses and nodules in units 5 and 11 were probably formed in or around these burrows. These pascichnid burrows are horizontal and are confined to layers near the middle of units 5 and 11. Pascichnid burrows in unit 13 are smaller (one inch in diameter) and show a more regular search pattern (Pl. 8, fig. 7). Since systematic search patterns are not exhibited clearly for any pascichnid found, these burrows may not be genuine pascichnid fossils.

Repichnid trails are abundant and show many variations of morphology. They are found in units 6, 10-B, 11-G, and 21-D. Figures 3 and 5 of Plate 8 show examples of repichnid trails in unit 6. In unit 11-G they are extremely abundant and are similar to the trace fossils shown in Plate 8, fig. 3. Units 6 and 10-B abound with repichnid trails (Pl. 8, fig. 5).

Fine-grained orange sandstones contain unidentifiable burrows in the upper massive portions. These burrows are approximately one inch in diameter, and they penetrate the rock at various angles. Deep weathering inhibits positive classification, although these burrows are probably domichnid fossils.

Vertical burrows like those illustrated in Plate 8, figure 10, are widespread throughout the clastic portion of the principal section. These small, vertical, irregularly oriented burrows can be found in any fine-grained purple arkose or very fine-grained orange sandstone (Text-fig. 3).

Bioturbation is also abundant in the principal section. Unit 15, for example, has mottled maroon-and-gray color with a "chewed-up" appearance that was undoubtedly caused by sediment-feeding organisms.

GEOCHEMISTRY

Some major and minor element analyses were made as spot checks of carbonate units to facilitate paleoecological interpretations and to correlate, if possible, trace-element abundance with fossil occurrence.

Table 2 summarizes data within the studied section (Text-fig. 7) and graphically shows chemistry of samples 2 through 13. Elemental abundance is shown in parts per million or in percentages.

Carbonate rocks were analyzed for the following: Mg, Ca, K, Al, Sr, Na, Mn, and Fe. That peaks of greatest elemental abundance are usually in mid-unit, and that graphs of most elements follow a common trend (Text-fig. 7) may be the result of ground water activity.

Magnesium is very stable and ranges in content from 0.4 to 12.53 percent (Table 2). In unit 11, highest and lowest values for magnesium are adjacent to each other.

Calcium content ranges from 17 to 43.38 percent (Table 2) and has expected high values since the analyses are of carbonate rocks. Graphs of potassium and aluminum show nearly identical trends, the latter being slightly more abundant. The highest values for both are in unit 15, and the lowest values are in unit 11. Aluminum ranges from 0.108 to 2.83 percent. The low value for potassium is .077 percent and the high, 2.07 percent (Table 2).

TABLE 2
Geochemical Results of Selected Units in Studied Section

Sample No.	Na ⁺	Ca	Sr ⁺	Mg	Si	Al	K	Fe	Mn ⁺
1	708	30.19	97	12.53	1.16	.351	.187	.270	4200
2	1756	19.70	93	9.85	6.64	1.320	1.070	.510	1760
3	2580	17.00	181	8.70	8.85	2.250	1.890	1.530	1600
4	2568	17.00	149	8.35	8.72	2.540	2.070	1.260	1650
5	952	35.50	542	.90	3.46	.980	.530	.745	925
6	303	21.70	93	12.30	1.38	.206	.126	.238	1800
7	1412	19.90	220	.90	19.70	1.050	.576	1.020	440
8	604	34.83	393	.60	3.98	.846	.472	.675	560
9	588	35.70	462	.60	3.45	.690	.428	.380	580
10	830	33.33	308	2.98	3.36	.960	.573	.604	1080
11	315	35.50	401	1.23	1.79	.544	.333	.396	850
12	687	27.00	247	5.12	4.64	1.200	.774	.780	650
13	222	38.38	466	.40	.82	.108	.077	.075	200
14	844	21.35	163	10.50	.34	.912	.483	.693	710
15	780	28.75	335	3.90	5.85	.920	.530	.836	1070
16	1412	29.62	308	1.13	8.80	1.230	.732	.702	450
17	297	31.51	378	1.32	6.22	.920	.538	.462	240
18	1366	24.33	346	2.02	17.50	2.830	1.410	1.790	350
19	761	24.81	167	8.60	4.86	.852	.455	.670	850
20	245	30.11	322	1.23	7.78	1.070	.612	.740	340

⁺ppm

Location of Samples. Sample no. 1, unit 20; sample no. 2, top of unit 15; sample no. 3, 5 feet from top of unit 15; sample no. 4, 6.5 feet from top of unit 15; sample no. 5, unit 13; sample no. 6, top of unit 11; sample no. 7, 9 feet from top of unit 11; sample no. 8, 4 feet from bottom of unit 11; sample no. 9, 3 feet from bottom of unit 11; sample no. 10, bottom of unit 11; sample no. 11, 1 foot from top of unit 7; sample no. 12, 4 feet from top of unit 7; sample no. 13, 2 feet from bottom of unit 7; sample no. 14, top of unit 5; sample no. 15, 4 feet from top of unit 5; sample no. 16, 7 feet from top of unit 5; sample no. 17, 8 feet from top of unit 5; sample no. 18, 15 feet from top of unit 5; sample no. 19, 11 feet from bottom of unit 5; sample no. 20, 6 feet from bottom of unit 5.

Strontium is present in very small quantities ranging from 93 to 542 parts per million. The abundance of strontium does not fluctuate markedly from unit to unit. The lowest value is in unit 11 and the highest value is in unit 13.

Sodium is most abundant in unit 15 and has both high and low values in unit 11. It ranges from 0.222 to 2.58 percent (Table 2).

Silicon shows a markedly high value in unit 11, probably caused by surrounding silicification of corals. Silicon ranges from 0.34 to 19.7 percent (Table 2).

Manganese ranges from 0.02 to 0.42 percent (Text-fig. 7) but is shown in Table 2 in parts per million. High values are prominent in units 11 and 13.

Iron ranges from 0.075 to 1.7 percent. A distinct low value occurs in unit 11, with high values in units 7, 11, and 15.

Sr/Ca, Ca/Mg, K/Al, and Fe/Mn ratios were calculated (Text-fig. 7) because they are thought to have some environmental significance. The Sr/Ca ratio is thought to be proportional to increasing paleosalinity (Turekian, 1955); the Ca/Mg ratio, inversely proportional to increasing paleotemperature (Chilinger, 1963); and the Fe/Mn ratio, perhaps proportional to increasing water depth (Baer, 1969).

The Sr/Ca ratio varies from unit to unit and fluctuates markedly within units (Text-fig. 7). Unit 7 shows a high ratio at its base, but the ratio decreases upwards, suggesting reduced salinity. Unit 11 has the most intra-unit fluctuations—as one would expect from the varied lithology and varied environments represented. Unit 13 has the highest Sr/Ca ratio and, if controlled by paleosalinity fluctuations, may indicate a wide variability in the chemistry of the Paradox Sea, particularly in the shore-zone areas.

Ca/Mg ratios follow the same general pattern as the Sr/Ca ratios, except in units 7 and 11 where their graphs intersect. High Ca/Mg ratios in units 7 and 11 may indicate low paleotemperature, while low Sr/Ca ratios, in the bottom of unit 7, at the top of unit 11, and in units 13 and 15, may indicate high paleotemperature with corresponding high paleosalinity.

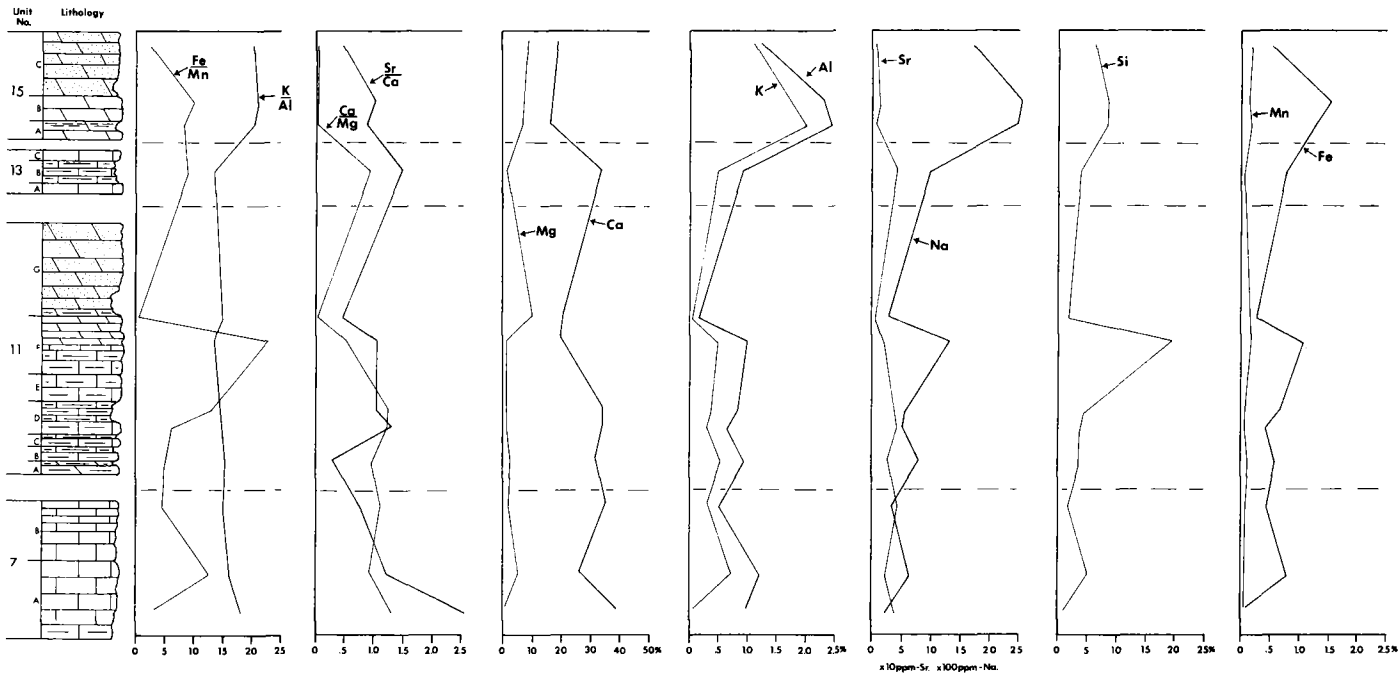
Fe/Mn ratio is anomalously high in unit 11 as compared with other ratios. High Fe/Mn ratios are found in mid-unit, which may indicate the deepest water or the farthest reaches of each transgression.

In comparing Text-fig. 7 with Text-figs. 5 and 6, fossil abundance is roughly correlative with trace-element abundance. Generally, brachiopods can be correlated with high values in K, Al, Na, Fe, and Mg and in the Sr/Ca and Ca/Mg ratios. Mollusks also have associated high values in Mg and in the Sr/Ca and Ca/Mg ratios. Secondary silicification of coral probably caused the high value for silicon in unit 11.

K/Al ratio was calculated to help interpret turbidity. The K/Al graph is stable for units tested. However, in unit 15 its value is higher than in other units, which probably indicates a higher turbidity for unit 15 than for other carbonate units.

CLIMATE AND GENERAL CONDITIONS

That the climate and the salinity, turbidity, energy, temperature, and depth of the water were changing during deposition of the studied area is evidenced



TEXT-FIGURE 7.—Distribution and ratios of trace elements in selected carbonate units.

by changes in the lithology, the sedimentary structures, the fauna, and the geochemistry of the rocks.

Climate during the time of deposition probably consisted of a short, torrential rainy season followed by a long dry season. Coarse- and fine-grained purple arkosic rocks are the products of a short, torrential rainy season, whereas freshness of arkoses and lack of shale, clay products, coal, and vegetation indicate an arid climate where weathering processes act at a reduced rate. Considering the amount of arkose available for weathering, there would be more clay deposits if the climate had been moist temperate or tropical.

Water salinity during the time of deposition probably fluctuated between fresh and hypersaline. The four sparry dolomites and two possible solution breccias indicate possible hypersaline water conditions. However, salinity during deposition of the dolomites generally was not high enough to preclude organic activity. Carbonate units 5 and 11 were probably deposited under marine saline conditions, as indicated by the presence of marine fossils. Coarse-grained purple arkoses are of fluvial origin and were probably deposited under freshwater conditions.

The degree of turbidity was controlled by a proximity to a clastic-depositing environment. The aurora of turbid water probably did not extend far from the clastic source because there are no thick clay deposits in the studied area which would indicate high turbidity. In open-marine carbonate deposits, clay is present as a thin coating on bedding-plane surfaces. These deposits are probably the result of suspended clay matter settling down over long periods of time. The small amounts of clay may also indicate relatively clear water conditions.

The water temperature was probably typical of arid climates. It was warm enough to allow deposition of CaCO_3 , yet cold enough to sustain highly diverse and complex communities of organisms. During the formation of sparry dolomites, water temperatures were probably warmest because water was shallow and circulation slow—as indicated by the presence of solution breccias and algae and by high Mg content (Table 2; Text-fig. 7). Water temperature was coldest in offshore environments and warmest in near-shore environments. Geochemical Ca/Mg ratios support this conclusion for carbonate units tested (Text-fig. 7).

There are subaerial, subaqueous, and intermittently exposed deposits within the studied locale. Water depth during deposition of coarse-grained purple arkoses was probably not as deep as the thickness of the thickest arkose, which is 40 feet. Channel depth was probably much shallower. Depth of water over very fine-grained orange sandstones and near-shore dolomites was probably never deeper than a few feet. That open-marine deposits were within the photic zone is indicated by the presence of common algae. Water depth could have been as much as 150 feet, but lithology and sedimentary structures generally do not indicate deposition in that depth of water. The water was probably much less than 100 feet deep.

Current direction, strength, and duration fluctuated a great deal within the principal section. Strong currents were probably responsible for depositing the coarse-grained purple arkoses into the Paradox Sea. Furthermore, deposition and water flow may have been continuous through a rainy season.

Small-scale current and oscillation ripple marks which are abundant in very fine-grained silty orange sandstones are indicative of weak water or

wind movements. Megaripples in tidal channel deposits indicate stronger currents (Pl. 2, fig. 8).

That the dominant paleocurrent direction is westerly and southerly is evidenced by paleocurrent data (Text-figs. 3, 4). Westerly transport direction probably originated from the slopes of the Uncompahgre Uplift (Text-fig. 2). That the southeasterly transport direction probably resulted from strong onshore or longshore currents originating from the northwest is evidenced by the coarse, immature nature of lithologies, the gradation from coarse to fine-grained textures along cross-bed sets, and the sedimentary structures associated with this paleocurrent direction. And that the southwesterly paleocurrent direction probably originated from weak longshore currents or eolian currents from the northeast is evidenced by the fine-grained, mature lithologies associated with this paleocurrent direction.

Evidence that the water energy of the tabular, cross-bedded orange sandstones was weaker than that for the arkoses is provided by the fine-grained composition of the orange sandstone deposits. And evidence that the carbonate and dolomitic deposits are products of low-energy environments is provided both by their dominantly micritic textures and by the absence of current-generated sedimentary structures.

FOSSIL HABITATS AND RELATIONSHIPS

That rugose corals thrived in an environment farthest from shore, in coldest, deepest, and clearest water of normal marine salinity, is attested to by surrounding carbonate lithologies, geochemistry, and fossil density and diversity.

The high density of rugose corals indicates that they were successful and stable in this environment. The lack of fossil diversity among the corals is probably due to the scarcity of nutrients that would have sustained other organisms.

Syringopora is found in various lithologies, which indicates that it was not restricted as were rugose corals but could live in many environments. *Syringopora* is often found surrounded by copious echinoid-spine debris, possibly suggesting that these two organisms were dependent upon one another in some way or were mutually controlled by some other environmental factor.

Syringopora and caninid corals are often found on top of small lophophyllid corals. The larger corals may have depended upon the smaller corals as a base for attachment.

Chonetes granulifer, a small, thin-shelled brachiopod (as in unit 11), was probably transported to where it is found in association with larger, more rugged organisms. The thin, dense layer of *Chonetes* found in unit 14 is probably a lag deposit.

Composita was probably an epifaunal organism, for it is found in living position in some limestone deposits. The species is thought to have been adaptable because it is found in a variety of lithologies.

It is also assumed that because large productid brachiopods, such as *Dictyoclostus* and *Echinoconchus*, are found in varied carbonate lithologies, they were also adaptable.

Juresania and *Marginifera*, the medium and small productid brachiopods, apparently lived in small clusters of a half-dozen individuals. They may

have exploited other brachiopods, such as *Neospirifer*, by attaching onto them.

Nuculana, a small pelecypod, is thought to have been an infaunal organism that lived in a low-energy, fine-grained, clastic environment, because *Nuculana* is found widely dispersed only in the shale of unit 14.

Wilkingia is an infaunal organism often found at the end of its burrow. The lithology in which it is found suggests a foul, inhospitable environment.

Bryozoa within units 11-C and D probably represent an adaptation to increasingly high levels of water energy. Bryozoa in these rocks change from smaller forms to larger, massive forms capable of surviving in more rugged conditions.

Each assemblage is thought to represent the basic members of a living community. Some rare organisms were undoubtedly transported, but it is believed, because of the fine-grained, micritic limestone lithology of the surrounding matrix, the lack of size grading among fossils, the lack of abrasion, and the lack of sedimentary structures or other evidence of strong currents, that the assemblages are essentially *in situ*, representative of living communities.

Fossils found closely associated with each other in the principal section are grouped into fossil assemblages which, based on surrounding lithologies, can be classified according to relative distance from shore or distance from clastic source.

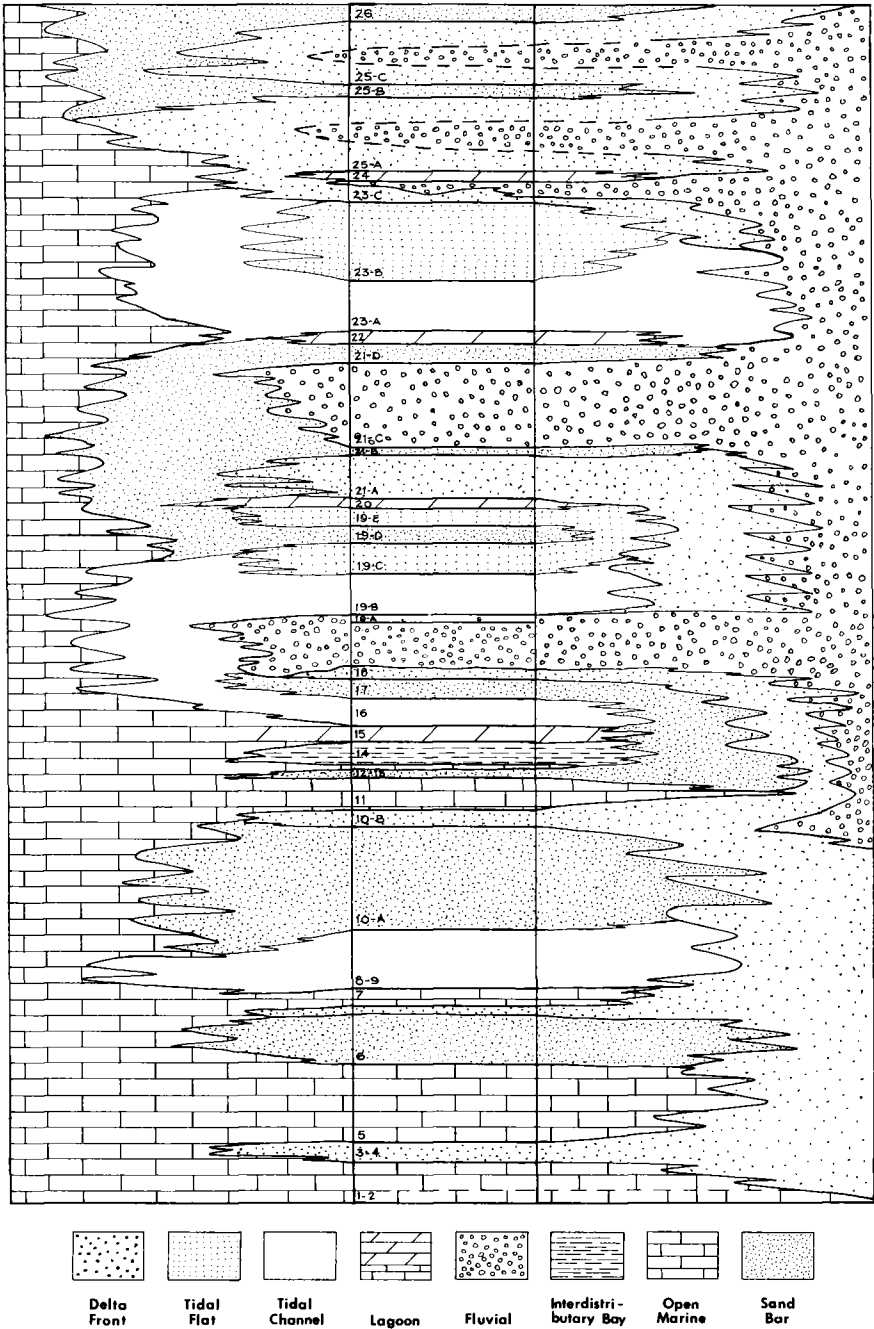
Text-fig. 9 is a hypothetical plan view showing fossil assemblage interrelationships superimposed on a sedimentary model. Biostromal algae, rugose corals, and *Syringopora* corals were farthest from shore. Closer to shore, abundant brachiopods are found in more clastic, higher-water-energy environments. Within the shore-zone complex of environments, gastropod- and pelecypod-dominated fossil assemblages are found in quiet-water-energy environments. *Syringopora* and biohermal algae also survived close to shore.

Furthermore, trace fossils show variations from near-shore to marine or offshore environments. Most near-shore trace fossils are small, irregularly spaced, vertical burrows. Further from shore, the deposits are extensively bioturbated and contain domichnid-type burrows. In subaqueously deposited clastic rocks, repichnid trails are prominent, and in offshore marine carbonate deposits, large in-sediment horizontal burrows of pascichnid type are found. Pascichnia are also present in near-shore carbonate environments of pelecypod-dominated fossil assemblages.

SEDIMENTARY ENVIRONMENTS

Deposits in the studied locale are classified into sedimentary environments based on the abundance and types of sedimentary structures, paleocurrent direction, lithology, fossils, sequence of occurrence, and integration with all other types of deposits found in the studied locale.

Coarse-grained purple arkoses, because of their abundant trough cross-bedding, immature lithology (which has been reworked very little), westerly paleocurrent direction, domichnid fossils, abundant vertical burrows, and associated lithologic units (near-shore and marine deposits), are thought to have been deposited by fluvial agents at the interface of the Honaker Sea and its shoreline.

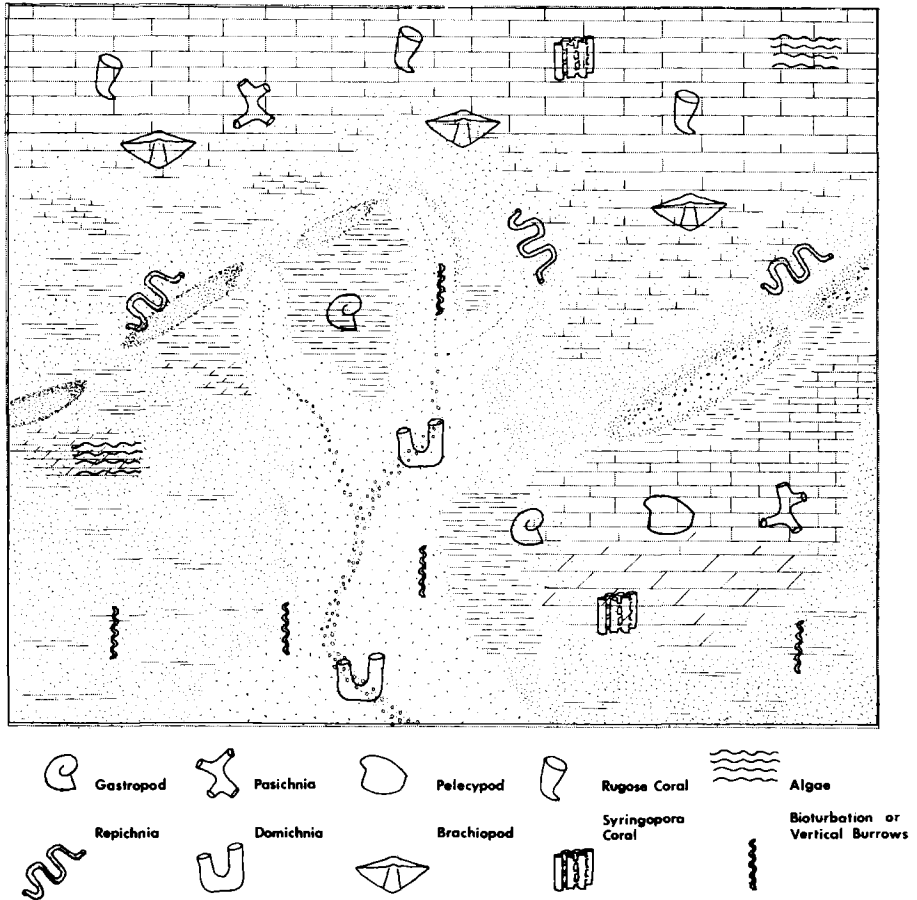


TEXT-FIGURE 8.—Diagram of rock units in studied section with superimposed sedimentary environments. Shows repetition and hypothetical intertonguing relationships of sedimentary environments. Note more marine environments at base becoming nonmarine at top.

Fine-grained purple arkoses are probably delta-front deposits, as evidenced by their subaqueous repichnid fossils and vertical burrows; immature lithology; contorted bedding, composed of sparse cross-bedding and abundant flat-bedding; and their relationships to the coarse-grained purple arkoses and carbonate deposits.

Tabular, cross-bedded orange sandstones are probably reworked delta material transformed into eolian dunes, barrier bars, or sand plains in front of or transgressing tidal-flat deposits. This conclusion is based on their mature lithology, tabular cross-bedding, southwesterly paleocurrent direction, trace-fossil occurrence, and relationships to purple arkoses and very fine-grained, silty orange sandstones.

Although very fine-grained, silty orange sandstones could be products of various other environments, here they are thought to be tidal-flat deposits



TEXT-FIGURE 9.—Sedimentary model, showing hypothetical delta complex and laterally equivalent marine carbonates with fossil distribution superimposed.

because of their abundant mudcracks, various ripple marks, mature lithology, flat bedding, and associated deposits.

Megarippled, fine-grained purple arkoses are probably tidal-channel and/or lower tidal-flat deposits. They are highly burrowed and contain various ripple marks, thin arkosic conglomerates, and small thin layers of limestone.

Coarse-grained white arkoses are thought to be washover fans associated with beach or bar deposits. They grade laterally into fine-grained, dark silty sandstone of probable lagoon or tidal-flat origin. Their southeasterly paleo-current direction, tabular cross-bedding, immature lithology, and relationships with other quiet-water-energy deposits support this conclusion. Coarse-grained white arkoses are probably the result of strong currents reworking channel deposits.

That the maroon-and-gray silty shale of unit 14 is probably an interdistributary bay or clastic lagoon deposit is attested to by its lithology, fossil assemblages and lack of current-generated sedimentary structures.

Thin carbonate deposits such as unit 13, because of their lithology, fossil assemblage, associated deposits, and lack of sedimentary structures, are thought to be carbonate-mud lagoon- or delta-associated, quiet-water deposits.

Carbonate deposits with characteristic marine fossils probably represent offshore, marine environments.

Sparry dolomites are shallow-water, subtidal to supratidal deposits where large populations of sediment-feeding organisms, probably arthropods, lived. These deposits are commonly found associated with tidal flats and carbonate mud lagoons.

In Text-figure 10, sedimentary environments are spatially oriented with sedimentary structures superimposed. For the purposes of this study, sedimentary environments have been grouped into a system combining the deltaic and the longshore processes included within a delta complex. Types and sequences of environments within the delta complex are listed below, beginning with onshore environments and ending with farthest-offshore environments:

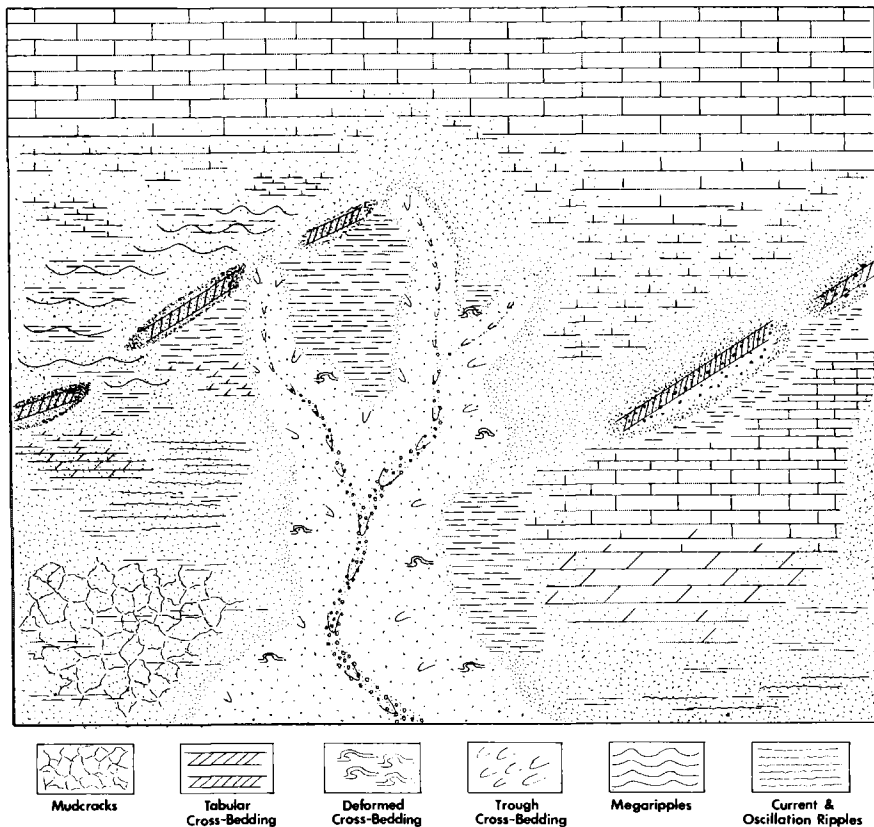
distributary channel	
tidal flat	
shallow water dolomite (subtidal to supratidal)	
clastic-dominated lagoon	} or interdistributary bay
carbonate mud lagoon	
barrier bar or marine bar	
fore bar sand	
open marine carbonate mud	

The entire sequence rarely runs to completion. Normally, only partial sequences or deposits out of order are seen, and sequences are ordinarily bounded by marine carbonate units.

SEDIMENTARY MODEL

The sedimentary model is based in two facts: the Paradox Basin was subsiding, and the Uncompahgre Uplift was rising. The sedimentary model also assumes that sedimentation was produced and controlled by several laterally shifting delta complexes and marine shoreline processes.

An overview of the area would show numerous braided piedmont or alluvial streams intermittently carrying coarse-grained purple arkose basinward



TEXT-FIGURE 10.—Sedimentary model of delta complex and carbonate environments with superimposed distribution of sedimentary structures.

at several points along the Uncompahgre front. These streams deposited their load into the shallow Paradox Sea margin through small migrating delta systems. The deltas prograde into the sea until stream gradient becomes low and sedimentation exceeds subsidence, choking old channels and diverting the whole system to a new topographic low where the gradient is steeper (Fisher, 1969, p. 13). When a delta lobe or complex is abandoned, carbonate marine deposits cover the old delta complex as the basin subsides. Alternation of delta position will produce repetitive sequences of rock deposits. As numerous delta complexes migrated and coalesced, the widespread effect of continuous lateral deposition was produced.

Repetition of environments can be seen upward through the principal section, gradually changing from marine- to nonmarine-dominated deposits (Text-fig. 8).

Text-figures 9 and 10 are diagrams of a hypothetical migrating delta lobe and of hypothetical carbonate environments with superimposed fossils and sedimentary structures.

Open-marine carbonate rocks alternate vertically with delta-system deposits and can be laterally continuous or discontinuous. That is, marine carbonate rocks grade into deltaic rocks shoreward or weave over and under entire systems in a direction parallel to the strike of the Uncompahgre front.

SUMMARY

The overall environment of deposition in the studied locale was part of a shallow marine-water, carbonate basin with numerous small delta complexes migrating back and forth along the shore zone, resulting in repetitive sedimentation.

Sedimentary environments that make up the delta complex and carbonate realms are distributary or fluvial channels, delta-front deposits, barrier-bar or beach deposits, tidal-flat deposits, tidal-channel deposits, and open-marine deposits.

Fossils were environmentally controlled, occupying ecological niches at certain distances from the shore. The most dominant fossils from the shore seaward are: gastropods, pelecypods, brachiopods, coral, and algae. By means of their type and abundance, trace fossils delimit the environment for most clastic rocks. From the shore seaward, they are most commonly vertical burrows, bioturbation, domichnia, repichnia, and pascichnia. The climate was arid, interrupted only by a short wet season. Vegetation was sparse. The Paradox Sea was a low-water-energy environment, mostly clear and warm, with normal marine salinity.

APPENDIX

Measured Stratigraphic Section

<i>Unit</i>	<i>Description</i>	<i>Feet/ Unit</i>	<i>Total Feet</i>
26	Sandstone: arkosic, medium-grained sand to fine pebble, very poorly sorted, gray white; larger tabular cross-bedding; ledge former	8'	597' 11"
25-C	Sandstone: arkosic, medium-grained sand to granule, poorly sorted, purple; trough and deformed cross-bedding common, flat bedding; slope former; domichnia	34'	589' 11"
25-B	Sandstone: quartzitic, silty to fine-grained sand, moderately sorted, orange; tabular cross-bedding, flat bedding; slope former	7'	555' 11"
25-A	Sandstone: arkosic, fine-grained sand to granule, purple; flat bedding, trough and deformed cross-bedding common; slope former; domichnia	40'	548' 11"
24	Dolomite: sucrosic, sandy, tan; secondary concretions of calcite; ledge former	4'	508' 11"
23-C	Sandstone: arkosic, very fine-grained sand to granule; upper portion is purple arkose, base is very fine-grained orange sandstone; trough cross-bedding, flat bedding; trace fossils	11'	504' 11"
23-B	Sandstone: quartzitic, silty to very fine-grained sand, orange; mudcracks, ripple marks, tabular cross-bedding; cliff former; abundant trace fossils	40'	493' 11"
23-A	Sandstone: arkosic, silty to granule size, purple; flat bedding, trough cross-bedding common; slope former; trace fossils	26'	453' 11"

Appendix 1 (Continued)

22	Dolomite: sucrosic, sandy, gray to gray red; secondary calcite concretions (fossil ghosts); ledge former; trace fossils	9'	427' 11"
21-D	Sandstone: quartzitic, silty to fine-grained sand, orange; flat bedding, tabular cross-bedding; undercut slope former; trace fossils	10'	418' 11"
21-C	Sandstone: arkosic, fine-grained sand to medium-grained pebbles; poor sorting; purple; trough cross-bedding; lenses of bioturbated siltstones; slope former	44'	408' 11"
21-B	Sandstone: quartzitic, silty to fine-grained sand, moderate sorting; tabular cross-bedding common, flat bedding; trace fossils	6'	364' 11"
21-A	Sandstone: arkosic, fine-grained sand to fine-grained pebble, poor sorting, purple; flat bedding, micro-cross-laminations, trough and deformed cross-bedding common; slope former; trace fossils	23'	358' 11"
20	Dolomite: sucrosic, sandy, tan; secondary calcite concretions; <i>Syringopora</i> , <i>Wilkingia</i> , <i>Straparollus</i> , trace fossils	3'	335' 11"
19-E	Sandstone: quartzitic, silty to medium-grained sand, orange, flat bedding, trough cross-bedding; undercut slope former; trace fossils	9' 6"	332' 11"
19-D	Sandstone: quartzitic, very fine-grained to fine-grained sand, orange; large tabular cross-bedding abundant at base; massive at top; cliff former; abundant trace fossils	9'	323' 5"
19-C	Sandstone: quartzitic with clay chips, silty to very fine-grained sand, moderate sorting, orange; flat bedding, numerous mud-cracks; slope former; abundant trace fossils	16'	214' 5"
19-B	Sandstone: arkosic, silty to granule size, moderate to poor sorting, orange and purple; massive and flat bedding in upper portion, trough cross-bedding common, possible mega-ripple marks; slope former, abundant trace fossils	22' 5"	298' 5"
19-A	Siltstone: quartzitic, clay to very fine-grained sand, brown; micro-cross-laminations; trace fossils	6'	276'
18	Conglomerate or sandstone: arkosic, medium-grained to very coarse gravel, very poorly sorted, purple; trough cross-bedding abundant; slope and cliff former	29'	270'
17	Sandstone: quartzitic, very fine- to medium-grained sand, deformed bimodal texture, orange; abundant tabular cross-bedding at base; cliff former; trace fossils at top	9'	241'
16	Sandstone: arkosic, silty to granule size, moderate to poor sorting, purple; trough cross-bedding, mega-ripple marks; trace fossils	13'	232'
15	Dolomite: sucrosic, sandy, red and gray; highly bioturbated; ledge and slope former; <i>Linoproductus</i> , <i>Orbiculoidea</i> , <i>Ptychomphalus</i> , <i>Straparollus</i> , <i>Echinocrinus</i> , arthropod, bioturbation	7'	219'
14	Shale: very fine-grained silt, gray red to light gray; covered slope; <i>Linoproductus</i> , <i>Chonetes</i> , <i>Chonetina</i> , <i>Cbaenomya</i> , <i>Aviculopecten</i> , <i>Permophorous</i> , <i>Pteronites</i> , <i>Pseudomonotis</i> (?) <i>Nuculana</i> , <i>Parallelodon</i> , <i>Euphemites</i> , <i>Bellerophon</i> , <i>Straparollus</i> , <i>Knightites</i> , <i>Pharkidonotus</i> , <i>Anomphalus</i> , bryozoans	12'	212'
13	Limestone: argillaceous, gray; usually covered ledge; <i>Neospirifer</i> , <i>Linoproductus</i> , <i>Marginiifera</i> , <i>Chonetes</i> , <i>Composita</i> , <i>Juresania</i> , <i>Aviculopecten</i> , <i>Limatula</i> , <i>Pseudomonotis</i> , <i>Limapecten</i> , <i>Myalina</i> , <i>Septimyalina</i> , <i>Acanthopecten</i> , <i>Schizodus</i> (?), <i>Euphemites</i> , <i>Worthenia</i> , <i>Pharkidonotus</i> , <i>Ditomophye</i> , <i>Echinocrinus</i> , <i>Derbyia</i> , <i>Lima</i> , <i>Bellerophon</i> , bellerophonid gastropods, <i>Edmondia</i> , <i>Wilkingia</i> , <i>Straparollus</i> , pascichnia	1' 9"	200'

Appendix 1 (Continued)

12	Sandstone: arkosic, medium to fine pebble size, white; abundant tabular cross-bedding	3'	198'	3"
11	Interbedded limestone and dolomite: argillaceous, gray; medium to thin bedded; cliff former. Sub-unit lithologies:			
	11-G Dolomitic, fine-grained quartzitic sandstone; quartzose sucrosic dolomite; argillaceous sucrosic dolomite; repichnia	6' 3"	195'	3"
	11-F Phylid dolomite; argillaceous micritic skeletal limestone; <i>Caninia</i> , <i>Lophophyllidium</i> , <i>Composita</i> , <i>Syringopora</i> , <i>Neospirifer</i> , <i>Dictyoclostus</i> , echinoid spines	2' 6"	189'	
	11-E Argillaceous micritic skeletal limestone; <i>Caninia</i> , <i>Lophophyllidium</i> , <i>Derbyia</i> , <i>Neospirifer</i> , <i>Echinoconchus</i> , <i>Dictyoclostus</i> , <i>Composita</i> , echinoid spines	1' 8"	186'	6"
	11-D Lithoclastic (quartz) micritic skeletal limestone; <i>Lophophyllidium</i> , <i>Neospirifer</i> , <i>Echinoconchus</i> , <i>Punctospirifer</i> , <i>Dictyoclostus</i> , <i>Marginifera</i> , <i>Chonetes</i> , <i>Delocrinus</i> , crinoid debris, demosponge, <i>Derbyia</i> , <i>Wellerella</i> , <i>Composita</i> , <i>Juresania</i> , <i>Bellerophon</i> , <i>Straparollus</i> , <i>Pharkidonotus</i> , <i>Ditomopyge</i>	2' 4"	184'	10"
	11-C Argillaceous micritic skeletal limestone; <i>Nautilus</i> , <i>Neospirifer</i> , <i>Echinoconchus</i> , <i>Chonetes</i> , <i>Composita</i> , <i>Juresania</i> , <i>Schizodus</i> , <i>Ditomopyge</i> , <i>Punctospirifer</i> , <i>Dictyoclostus</i> , <i>Marginifera</i> , <i>Derbyia</i> , <i>Wellerella</i> , <i>Wilkingia</i> , <i>Edmondia</i> , <i>Straparollus</i> , <i>Pharkidonotus</i>	10'	182'	6"
	11-B Argillaceous, skeletal, micritic limestone; solution breccia; <i>Neospirifer</i> , <i>Dictyoclostus</i> , <i>Marginifera</i> , <i>Wilkingia</i> , crinoid debris	9"	181'	8"
	11-A Argillaceous, bioclastic, fine-grained dolomite; fusulinid limestone; limey claystone; <i>Dictyoclostus</i> , <i>Triticites</i> , crinoid debris	9"	180'	11"
10-B	Sandstone: arkosic, fine-grained to very coarse-grained sand, purple; trough and deformed cross-bedding common at base of unit; undercut slope former	6'	180'	2"
10-A	Sandstone: quartzitic, silty to fine-grained sand, orange; abundant tabular cross-bedding, occasional deformed cross-bedding; trace fossils common; cliff former	29' 2"	174'	2"
9	Sandstone: interbedded arkosic and quartzitic, silty to coarse grained sand, orange; flat bedding, megaripple marks, trough cross-bedding; six-inch limestone layer in mid-unit; trace fossils	25'	145'	
8	Siltstone: quartzitic, silty to very fine-grained sand, purple and gray; massive; slope former	7'	120'	
7	Limestone: micritic, gray; solution breccia, intraformational conglomerate; thin bedded; cliff former; algae, echinoid spines, <i>Echinoconchus</i> , <i>Dictyoclostus</i> , <i>Pseudomonotis</i> , <i>Lino-productus</i> , <i>Composita</i> (?)	9' 6"	113'	
6	Sandstone: quartzitic and arkosic, very fine- to coarse-grained sand, white to purple; tabular deformed cross-bedding common; upper portion arkosic with deformed cross-bedding; lower portion flat bedded; fodinichnia, repichnia	32'	103'	6"
5	Limestone and dolomite: micritic and algal (biostromal), gray and green; flat bedded; cliff former; trace fossils, branching and sheeting bryozoan, <i>Neospirifer</i> , <i>Echinoconchus</i> , <i>Dicty-</i>			

Appendix 1 (Continued)

	<i>oclostus</i> , echinoid spines, <i>Caninia</i> , <i>Lophophyllidium</i> , <i>Syringopora</i> , <i>Composita</i> , <i>Echinocrinus</i>	40'	69'	6''
3 & 4	Sandstone: arkosic, silty to coarse-grained sand, gray; cross-bedding common, flat bedded	3'	6''	29'
2	Sandstone: quartzitic, fine- to medium-grained sand, tan; massive; rare fossil plants; cliff former	24'		26'
1	Sandstone: quartzitic, silty to fine-grained sand, brown; massive	2'		2'

REFERENCES CITED

- Baars, D. L., 1962, Permian System of the Colorado Plateau: Amer. Assoc. Petrol. Geol. Bull., v. 46, p. 149-218.
- Baer, J. L., 1969, Paleoecology of cyclic sediments of the lower Green River Formation, Central Utah: Brigham Young Univ. Geol. Studies, v. 16, pt. 1, 3-95.
- Baker, A. A., Dobbin, C. E., McKnight, E. T., and Reeside, J. B., 1927, Notes on the stratigraphy of the Moab region: Amer. Assoc. Petrol. Geol., v. 11, no. 8, p. 785-808.
- Baker, A. A., 1933, Geology and oil possibilities of the Moab district, Grand and San Juan Counties, Utah: U.S. Geol. Survey Bull. 841, 95 p.
- Chilinger, G. V., 1963, Ca/Mg and Sr/Ca ratios of calcareous sediments as a function of depth and distance from shore: Jour. of Sed. Pet., v. 33, no. 1, p. 236.
- Chronic, J., 1960, Late Paleozoic paleontology in the northern Paradox Basin: Four Corners Geol. Soc. Guidebook, 3rd Field Conf., p. 80-85.
- Cross, C. W., and Spencer, A. C., 1899, Description of the La Plata quadrangle: U.S. Geol. Survey Geol. Atlas, Folio 60, 14 p.
- , 1900, Geology of the Rico Mountains, Colorado: U.S. Geol. Survey 21st Ann. Report, pt. II, p. 115-165.
- Cross, C. W., and Howe, E., 1905, Redbeds of southwestern Colorado and their correlation: Geol. Soc. Amer. Bull., v. 16, p. 447-498.
- Cross, C. W., 1907, Stratigraphic results of reconnaissance in western Colorado and eastern Utah: Jour. Geol., v. 15, p. 634-679.
- Fisher, W. L., Brown, L. F., Scott, A. J., and McGowan, J. H., 1969, Delta systems in exploration for oil and gas: Texas Bureau Econ. Geol., Austin, 78 p.
- Newberry, J. S., 1876, Geological Report: in J. N. N. Macomb, Report of the exploring expedition from Santa Fe, New Mexico, to the junction of the Grand and Green rivers of the Great Colorado of the West in 1859: U.S. Army Engineer Dept., p. 9-118.
- Parr, C. J., 1965, A study of primary sedimentary structure around the Moab anticline, Grand County, Utah: unpub. M.S. thesis, Univ. of Utah, 102 p.
- Plumley, W. J., Risley, G. A., Graves, R. W., Jr., and Kaley, M. E., 1962, Energy index for limestone interpretation and classification: in W. E. Ham [ed], Classification of carbonate rocks, Amer. Assoc. Petrol. Geol. Mem. 1, p. 85-107.
- Seilacher, A., 1964, Biogenic sedimentary structures: in J. Imbrie, and N. Newell [eds.], Approaches to Paleoecology: John Wiley and Sons, Inc., New York, p. 296-316.
- Turekian, K., 1955, Paleoecologic significance of strontium-calcium ratio in fossils and sediments: Bull. Geol. Soc. Amer., v. 66, p. 155-158.
- Wengerd, S. A., and Matheny, M. L., 1958, Pennsylvanian System of the Four Corners region: Bull. Amer. Assoc. Petrol. Geol., v. 42, p. 2048-2106.
- Wengerd, S. A., 1962, Pennsylvanian sedimentation in the paradox Basin, Four Corners region: in C. C. Branson [ed.], Pennsylvanian Systems in the U. S.: Amer. Assoc. Petrol. Geol., p. 264-330.